DiiodoBodipy−StyrylBodipy Dyads: Preparation and Study of the Intersystem Crossing and Fluorescence Resonance Energy Transfer

ARTICLE *in* THE JOURNAL OF PHYSICAL CHEMISTRY A · JUNE 2015

Impact Factor: 2.69 · DOI: 10.1021/acs.jpca.5b03463 · Source: PubMed

5 AUTHORS, INCLUDING:

Yun Xie

Bowling Green State University

4 PUBLICATIONS **5** CITATIONS

SEE PROFILE

THE JOURNAL OF PHYSICAL CHEMISTRY A

Article

pubs.acs.org/JPCA

Diiodobodipy-styrylbodipy Dyads: Preparation and Study of the Intersystem Crossing and Fluorescence Resonance Energy Transfer

Zhijia Wang,[†,§] Yun Xie,[‡,§] Kejing Xu,[†] Jianzhang Zhao,*[,†] and Ksenija D. Glusac*[,‡]

[†]State Key Laboratory of Fine Chemicals, School of Chemical Engineering, Dalian University of Technology, E-208 West Campus, 2 Ling-Gong Road, Dalian 116024, P. R. China

[‡]Department of Chemistry, Center for Photochemical Sciences, Bowling Green State University, Bowling Green, Ohio 43403, United States

Supporting Information

ABSTRACT: 2,6-Diiodobodipy-styrylbodipy dyads were prepared to study the competing intersystem crossing (ISC) and the fluorescence-resonance-energy-transfer (FRET), and its effect on the photophysical property of the dyads. In the dyads, 2,6-diiodobodipy moiety was used as singlet energy donor and the spin converter for triplet state formation, whereas the styrylbodipy was used as singlet and triplet energy acceptors, thus the competition between the ISC and FRET processes is established. The photophysical properties were studied with steady-state UV−vis absorption and fluorescence spectroscopy, electrochemical characterization, and femto/nanosecond time-resolved transient absorption spectroscopies. FRET was confirmed with steady state fluorescence quenching and fluorescence excitation spectra and ultrafast transient absorption spectroscopy (k_{FRET} = 5.0 × 10^{10} s^{-1}). The singlet oxygen quantum yield (Φ_Δ = 0.19) of the dyad was reduced as compared with that of the reference spin converter (2,6-diiodobodipy, Φ_Δ = 0.85), thus the ISC was substantially inhibited by FRET. Photoinduced intramolecular electron transfer (ET) was studied by electrochemical data and fluorescence quenching. Intermolecular triplet energy transfer was studied with nanosecond transient absorption spectroscopy as an efficient (Φ_{TTET} = 92%) and fast process (k_{TTET} = 5.2 × 10^4 s^{-1}). These results are useful for designing organic triplet photosensitizers and for the study of the photophysical properties.

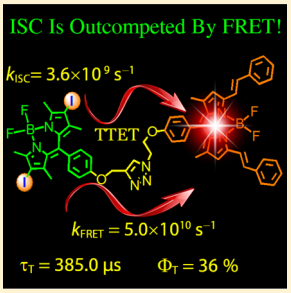

INTRODUCTION

Triplet photosensitizers (PSs) have been widely used in photocatalysis,[1−6] photodynamic therapy,[7−15] molecular probes,[16] triplet−triplet annihilation (TTA) upconversion,[17,18] and photovoltaics.[19] However, the conventional triplet PSs suffer from some common drawbacks, such as the difficulty to modify the molecular structures, weak absorption of visible light, and short-lived triplet excited states.[14,15] These photophysical features are disadvantages for applications of the triplet PSs, because intermolecular triplet state energy transfer (EnT) or electron transfer (ET) is very often involved in the photophysical processes initiated by triplet PSs.[15] Low concentration of the PSs at triplet excited state and short-lived triplet state are detrimental to the intermolecular EnT and ET processes.

In order to address these challenges, recently we and other groups prepared series of new triplet PSs that show strong absorption of visible light and long-lived triplet excited states, including bodipy-derived organic triplet PSs (by utilization of the heavy atom effect),[20,21] or by application of the new concept of intramolecular spin converter[22−27] and visible light-harvesting organic chromophore-containing Pt(II), Ir(III), Ru(II), and Re(I) complexes.[15,19,28] These compounds are more efficient for applications in TTA upconversion,[29] singlet oxygen ($^1O_2$) photosensitizing,[30] and photoredox catalytic organic reactions,[31−34] than the conventional triplet photosensitizers. However, to date these new triplet PSs still suffer from a drawback, that is, the molecular structures are based on monochromophore protocol. As a result, there is usually only one major absorption band in the visible spectral region, which is unable to efficiently harvest the energy of broadband visible light photoexcitation, such as solar light.[14,15] While broadband visible light-absorbing dyads or triads have been investigated,[35,36] those compounds were not designed for triplet PSs purpose, rather, they were for singlet excited state-related studies, such as fluorescence, and very often no triplet excited state was produced by these dyads/triads.[35−43] The most popular broadband visible light-absorbing chromophore dyads are based on the fluorescence-resonance-energy-transfer (FRET, or more precisely, RET) effect. However, for these FRET chromophore dyads/triads, the purpose is to fluoresce, not for formation of triplet excited state.[35−43]

Recently, we prepared RET-based broadband visible light absorption chromophore dyads and triads.[33,44−46] These new PSs show strong broadband absorption in visible spectra region and long-lived triplet excited states (triplet excited state lifetime is up to 100 μs). But the photophysical properties of these multichromophore triplet PSs are far from fully explored. Interesting photophysical processes were observed for these triplet PSs. For example, forward singlet EnT from the visible

Received: April 10, 2015
Revised: June 1, 2015
Published: June 3, 2015

DOI: 10.1021/acs.jpca.5b03463
J. Phys. Chem. A 2015, 119, 6791−6806

light-harvesting energy donor to the singlet energy acceptor (also the spin converter), as well as backward triplet EnT were observed for bodipy-diiodobodipy dyads.[44] Moreover, bodipy dyads/triads were studied as molecular logic gates, with production of $^1O_2$ as a unique output.[47,48] However, the photophysical properties of these multichromophore triplet PSs were not studied in detail with time-resolved transient absorption spectroscopy. Photoinduced intramolecular ET of the dyad or triad triplet PSs was not studied. ET is detrimental for triplet state formation, given the energy level of the charge transfer state (CTS) is lower than the T_1 state, as a result, the photoexcitation energy will be funneled to the CTS and no triplet excited state can be formed.[49,50] Furthermore, the singlet energy acceptors in the reported broadband absorbing triplet PSs usually play the role of a spin converter.[15,32,44,46] However, the alternative molecular structural profile (i.e., the singlet energy donor as the spin converter in a dyad with FRET), has not been studied (Figure 1). Previously, it was proposed that

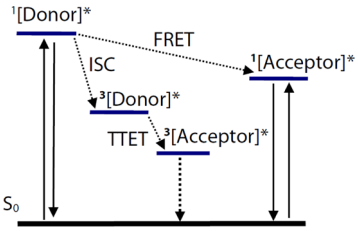

Figure 1. Simplified Jablonski diagram for the competing ISC and FRET. Note the T_1 state of the dyads studied in this paper is localized on the energy acceptor (styrylbodipy) moiety.

the ISC is able to be completely inhibited by FRET,[47] but the photophysical process was not studied in detail with the femto- or nanosecond transient absorption spectroscopy. Competing ISC and FRET was rarely studied with organic dyads.[51−53] Previously, we found that the ISC is unable to be efficiently competed by FRET in bodipy-PBI (PBI = perylenebisimide) triad and bodipy-rhodamine dyads.[51,52] Moreover, the overlap of the steady-state absorption bands of the components of bodipy-PBI triad or the bodipy-rhodamine dyad is significant,[51,52] thus the assignment of the nanosecond transient absorption band is difficult. In addition, strong photoinduced electron transfer (PET) effect was observed in the naphthalenediimide triad system,[53] which makes it difficult to draw the conclusion that ISC is inhibited by FRET. Therefore, much room is left and more multichromophore photosensitizers are needed to fully explore the competition of FRET and ISC.

In order to address the above challenges, herein, we prepared bodipy dyads as triplet PSs (**B-1** and **B-2**, Scheme 1) to study the competition of ISC and FRET. In these dyads, the 2,6-diiodobodipy part is a visible light-harvesting unit and singlet energy donor, as well as the spin converter, which is responsible for production of triplet excited state upon photoexcitation.[15] The singlet energy acceptor is the styrylbodipy unit, for which the absorption band overlaps with the emission band of the diiodobodipy unit, thus FRET is envisaged, and competition between the ISC and FRET is established. The styrylbodipy unit is devoid of any ISC capability.[54] Different singlet energy acceptors were used in **B-1** and **B-2** (Scheme 1). The photophysical property of the dimethylaminostyrylbodipy in **B-2** can be switched with acid, by protonation of the Me_2N-group. The protonation will change the property of the triplet state of the styrylbodipy moiety thus offering additional switchability concerning triplet state manifold, which was very rarely studied.[49,50] Upon photoexcitation into the singlet energy donor, multiple photophysical processes will be initiated for these dyads, such as the ISC of the iodobodipy part and the competing FRET from the diiodobodipy to the styrylbodipy part,[47] as well as the photoinduced ET.[50] The photophysical processes of the dyads were studied with steady state and femto- and nanosecond transient absorption spectroscopy and electrochemical characterization. A reference dyad with no iodination of the bodipy unit was prepared for elucidating the photophysical properties (**B-3**, Scheme 1).

EXPERIMENTAL SECTION

General Methods. UV−vis absorption spectra were taken on a HP8453 UV−vis spectrophotometer. Fluorescence spectra were recorded on Shimadzu RF-5301PC spectrofluorometer. Luminescence lifetimes were measured on a OB920 fluorescence/phosphorescence lifetime instrument (Edinburgh, U.K.).

Synthesis and Characterization. *Synthesis of the Compound B-1.* Under N_2 atmosphere, compounds **4** (58.0 mg, 0.1 mmol) and **8** (76.0 mg, 0.12 mmol) were dissolved in mixed solvent $CHCl_3$/EtOH/H_2O (23 mL, 10:0.8:0.8, v/v), then the mixture was stirred at room temperature (RT). One drop of Et_3N was added, and the mixture was stirred for 5 min. Then sodium ascorbate (20 mg) and $CuSO_4{\cdot}5H_2O$ (10 mg) were added. The mixture was stirred at RT for 48 h. Then water was added, and the organic layer was collected and dried over anhydrous $MgSO_4$. The solvent was evaporated under reduced pressure. The crude product was purified using column chromatography (silica gel, dichloromethane) to give a dark solid. Yield: 80 mg (66%). Mp: 147.0−150.0 °C. ^{1}H NMR (400 MHz, $CDCl_3$): δ = 7.94 (s, 1H), 7.76 (s, 1H), 7.72 (s, 1H), 7.64 (d, 4H, J = 8.0 Hz), 7.42−7.39 (m, 4H), 7.32 (t, 2H, J = 8.0 Hz), 7.28 (s, 2H), 7.24 (s, 2H), 7.16 (s, 4H), 7.02 (d, 2H, J = 8.0 Hz), 6.64 (s, 2H), 5.30 (s, 2H), 4.86 (t, 2H, J = 4.0 Hz), 4.49−4.46 (m, 2H), 2.64 (s, 6H), 1.47 (d, 12H, J = 16.0 Hz). ^{13}C NMR (125 MHz, $CDCl_3$): δ = 158.2, 157.3, 155.7, 151.6, 144.1, 142.6, 141.0, 140.2, 137.5, 135.5, 135.3, 132.6, 130.6, 129.8, 128.9, 128.2, 127.9, 127.7, 127.4, 126.5, 126.4, 123.1, 118.2, 116.8, 114.7, 114.0, 61.1, 48.9, 37.7, 28.6, 16.1, 13.9. MALDI-HRMS($C_{57}H_{49}B_2F_4I_2N_7O_2$): calcd, m/z = 1215.2160; found, m/z = 1215.2175.

Synthesis of the Compound B-2. Under N_2 atmosphere, **5** (54 mg, 0.1 mmol) and **8** (76.0 mg, 0.12 mmol) were dissolved in mixed solvent $CHCl_3$/EtOH/H_2O (23 mL, 10:0.8:0.8, v/v), then the mixture was stirred at RT, a drop of Et_3N was added, and the mixture was stirred for 5 min. Then sodium ascorbate (20 mg) and $CuSO_4{\cdot}5H_2O$ (10 mg) were added. The mixture was stirred at RT for 48 h. Then water was added, the organic layer was collected and dried over $MgSO_4$. The solvent was evaporated under reduced pressure. The crude product was further purified using column chromatography (silica gel, dichloromethane) to give a dark solid. Yield: 58 mg (50%). Mp: 188.0−191.0 °C. ^{1}H NMR (400 MHz, $CDCl_3$): δ = 7.95 (s, 1H), 7.53 (d, 2H, J = 8.0 Hz), 7.26 (s, 5H), 7.23 (d, 2H, J = 8.0 Hz), 7.16 (s, 3H), 7.00 (d, 2H, J = 8.0 Hz), 6.60 (s, 1H), 5.97 (s, 1H), 5.30 (s, 2H), 4.87 (t, 2H, J = 4.0 Hz), 4.47 (t, 2H, J = 4.0 Hz), 3.05 (s, 3H), 2.64 (s, 9H), 2.18 (s, 3H), 1.43 (s, 12H). ^{13}C NMR (125 MHz, $CDCl_3$): δ = 157.7, 156.6, 155.1, 153.3, 151.3, 149.5, 143.7, 142.0, 141.1, 139.7, 139.0, 136.7, 136.3, 131.8, 130.1, 128.4, 127.7, 127.1, 125.8, 123.0, 122.6, 118.9,

DOI: 10.1021/acs.jpca.5b03463
J. Phys. Chem. A 2015, 119, 6791−6806

Scheme 1. Synthesis of the Triplet Photosensitizers B-1, B-2, and Reference B-3[a]

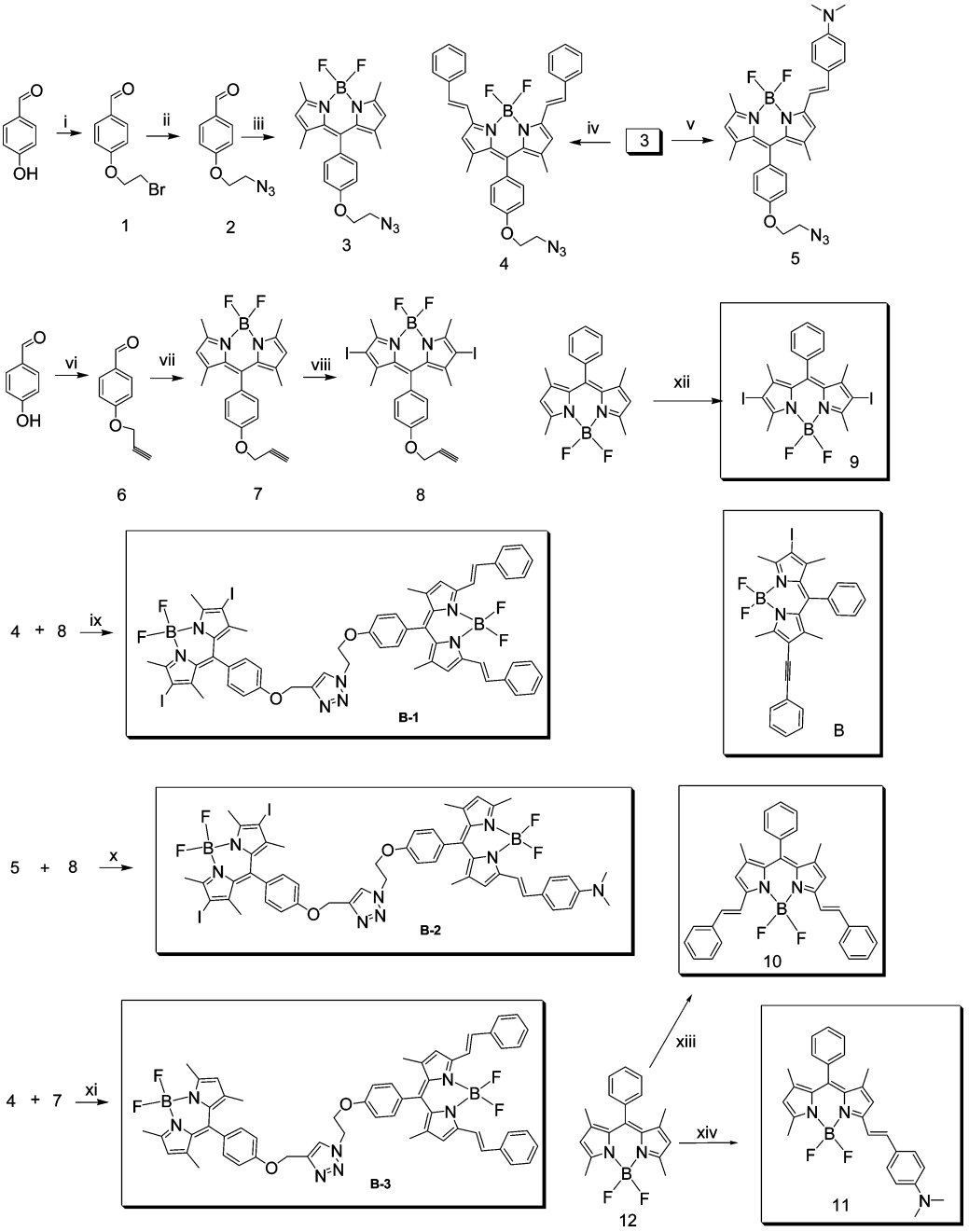

[a](i) 1,2-Dibromoethane, K_2CO_3, ethyl alcohol, 80 °C reflux, 24 h in Ar, 61%. (ii) NaN_3, DMF, 100 °C, 2 h, in Ar, 90%. (iii) 2,4−dimethylpyrrole, trifluoroacetic acid, DDQ, TEA, $BF_3{\cdot}Et_2O$, rt, 2 h, in Ar, 12%. (iv) Benzaldehyde, acetic acid, piperidine, DMF, 6 min, 150 °C, in Ar, 45%. (v) 4-*N*,*N*-dimethylbenzaldehyde, acetic acid, piperidine, toluene, 125 °C, 24 h, 25%. (vi) Propargyl bromide, K_2CO_3, DMF, 70 °C reflux, 6 h in Ar, 87%. (vii) 2,4-Dimethylpyrrole, trifluoroacetic acid, DDQ, TEA, $BF_3{\cdot}Et_2O$, rt, 2 h, in Ar, 16%. (viii) Dry DCM, *N*-Iodosuccinimide, rt, 12 h, 62%. (ix) Et_3N, $CuSO_4{\cdot}5H_2O$, and sodium ascorbate, 48 h, at rt, in Ar, 66%. (x) Et_3N, $CuSO_4{\cdot}5H_2O$, and sodium ascorbate, 48 h, at rt, in Ar, 50%. (xi) Et_3N, $CuSO_4{\cdot}5H_2O$, and sodium ascorbate, 48 h, at rt, in Ar, 55%. (xii) Dry DCM, *N*-iodosuccinimide, rt, 12 h, 65%. (xiii) DMF, benzaldehyde, acetic acid, piperidine, microwave irradiation, 5 min, in Ar, 60%. (xiv) 4-*N*,*N*-dimethylbenzaldehyde, toluene, acetic acid, piperidine, reflux, 24 h in Ar, 22%.

116.2, 114.0, 113.3, 110.5, 64.7, 60.5, 48.3, 38.7, 28.1, 15.6, 14.4, 13.4, 12.9. MALDI-HRMS($C_{52}H_{50}B_2F_4I_2N_8O_2$): calcd, m/z = 1170.2269; found, m/z = 1170.2292.

Synthesis of the Compound ***B-3***. Under N_2 atmosphere, **4** (58 mg, 0.1 mmol) and **7** (38 mg, 0.1 mmol) were dissolved in mixed solvent $CHCl_3$/EtOH/H_2O (23 mL, 10:0.8:0.8, v/v), then the mixture was stirred at RT. One drop of Et_3N was added, and the mixture was stirred for 5 min. Then sodium ascorbate (20 mg) and $CuSO_4{\cdot}5H_2O$ (10 mg) were added. The mixture was stirred at RT for 48 h. Then water was added, the organic layer was collected and dried over $MgSO_4$. The solvent was evaporated under reduced pressure. The crude product was further purified using column chromatography (silica gel, dichloromethane) to give a dark solid. Yield: 53 mg (55%). Mp: 174.0−178.0 °C. ^{1}H NMR (500 MHz, $CDCl_3$): δ = 7.93 (s, 1H), 7.76 (s, 1H), 7.72 (s, 1H), 7.64 (d, 3H, J = 5.0 Hz), 7.42−

DOI: 10.1021/acs.jpca.5b03463
J. Phys. Chem. A 2015, 119, 6791−6806

7.39 (m, 4H), 7.34−7.31 (m, 2H), 7.28 (s, 3H), 7.25 (d, 2H, J = 10.0 Hz), 7.21 (d, 2H, J = 10.0 Hz), 7.14 (d, 2H, J = 10.0 Hz), 7.02 (d, 2H, J = 10.0 Hz), 6.65 (s, 2H), 5.98 (s, 2H), 5.28 (s, 2H), 4.86 (t, 2H, J = 5.0 Hz), 4.47−4.46 (m, 2H), 2.55 (s, 6H), 1.47 (s, 6H), 1.43 (s, 6H). ^{13}C NMR (125 MHz, $CDCl_3$): δ = 159.0, 158.5, 155.6, 152.8, 143.9, 143.1, 142.2, 141.7, 138.7, 136.7, 136.5, 133.8, 131.9, 130.1, 129.5, 129.1, 128.9, 128.6, 127.9, 127.7, 124.3, 121.4, 119.4, 118.0, 115.6, 115.2, 66.5, 62.2, 50.1, 29.9, 15.1, 14.8. MALDI-HRMS($C_{57}H_{51}B_2F_4N_7O_2$): calcd, m/z = 963.4226; found, m/z = 963.4202.

Synthesis of the Compound ***9***. Bodipy (1.3 g, 4 mmol) was dissolved in dry CH_2Cl_2 (200 mL), then *N*-iodo-succinimide (NIS. 2.25 g, 10 mmol) in anhydrous CH_2Cl_2 (100 mL) was added. Then the mixture was stirred at RT for 12 h. The solvent was removed under reduced pressure, and the crude product was purified by column chromatography (silica gel, dichloromethane: hexane = 1:2, v/v) to give a red solid. Yield: 1.5 g (65%). ^{1}H NMR (400 MHz, $CDCl_3$): 7.54−7.51 (m, 3H), 7.26−7.24 (m, 2H), 2.65 (s, 6H), 1.39 (s, 6H).

Synthesis of the Compound ***10***. Under Ar atmosphere, bodipy (64 mg, 0.2 mmol) was dissolved in dry DMF (5 mL). Benzaldehyde (80 μL, 0.8 mmol) was added, followed by acetic acid (6 drops) and piperidine (6 drops). The mixture was subjected to microwave irradiation (5 min, 150 °C, 1 min prestirring). After removal of the solvent under reduced pressure, the mixture was purified by column chromatography (silica gel, dichloromethane: hexane = 1:1, v/v) to give a deep purple solid. Yield: 60 mg (60%). ^{1}H NMR (400 MHz, $CDCl_3$): δ = 7.78 (s, 1H), 7.74 (s, 1H), 7.66 (d, 4H, J = 8.0 Hz), 7.51 (d, 3H, J = 4.0 Hz), 7.41 (t, 4H, J = 8.0 Hz), 7.35 (d, 4H, J = 8.0 Hz), 7.29 (s, 1H), 7.25 (s, 1H), 6.66 (s, 2H), 1.45 (s, 6H). MALDI-HRMS ($C_{33}H_{27}BF_2N_2$): calcd, m/z = 500.2235; found, m/z = 500.2213.

Synthesis of the Compound ***11***. Under Ar atmosphere, a mixture of bodipy (32 mg, 0.1 mmol), 4-*N*,*N*-dimethylbenzaldehyde (62 mg, 0.4 mmol) were dissolved in dry toluene (15 mL), then acetic acid (1.5 mL) and piperidine (1.5 mL) were added. The mixture was refluxed for 24 h at 125 °C. After completion of the reaction, the mixture was cooled to room temperature. Water (75 mL) was added, and the mixture was extracted with dichloromethane (3 × 100 mL). After removal of the solvent under reduced pressure, the mixture was purified by column chromatography (silica gel, dichloromethane) to give a deep black solid. Yield: 10 mg (22%). ^{1}H NMR (400 MHz, $CDCl_3$): δ = 7.52−7.47 (m, 5H), 7.31 (t, 2H, J = 4.0 Hz), 7.26−7.23 (m, 4H), 6.60 (s, 1H), 5.97 (s, 1H), 3.03 (s, 6H), 2.59 (s, 3H), 1.42 (d, 6H, J = 16.0 Hz).

Cyclic Voltammetry Curves. The cyclic voltammetry curves were recorded by CHI 600E electrochemical workstation (CHI instruments, Inc. Shanghai, China). In N_2 saturated CH_3CN containing a 0.10 M Bu_4NPF_6 as supporting electrolyte; counter electrode is Pt electrode; working electrode is glassy carbon electrode; $Ag/AgNO_3$ couple as the reference electrode. c [Ag^+] = 0.1 M. 1.0 mM compounds in CH_3CN, 20 °C. Scan rates: 100 mV/s. Ferrocene (Fc) was used as an internal reference.

Nanosecond Transient Absorption Spectroscopy. Nanosecond time-resolved transient difference absorption spectra were recorded on a LP920 laser flash photolysis spectrometer (Edinburgh Instruments, UK). The solutions were purged with N_2 for 30 min before measurement. The samples were excited with a nanosecond pulsed laser (OPOLette 355II, wavelength tunable in the range of 410−2400 nm), and the transient signals were recorded on a Tektronix TDS 3012B oscilloscope.

Femtosecond Transient Absorption Spectroscopy. The 800 nm laser pulses were produced at a 1 kHz repetition rate by a mode-locked Ti:sapphire laser and regenerative amplifier (Hurricane, Spectra-Physics). The output from the Hurricane was split into pump (85%) and probe (10%) beams. The pump beam was fed into an optical paramagnetic amplifier (OPA-400, Spectra Physics) to obtain the desired excitation wavelength. The energy of the pump beam was 100 nJ/pulse. The probe beam was focused into a two-dimensional translated 4 mm CaF_2 crystal for white light continuum probe beam between 350 and 800 nm. The flow cell (Starna Cell Inc. 45-Q-2, 0.9 mL volume with 2 mm path length), pumped by a variable flow Mini-Pump (Control Company), was used to prevent photodegradation of the sample. After passing through the cell at the magic-angle geometry, the continuum was coupled into an optical fiber and input into a CCD spectrometer (Ocean Optics, S2000). The data acquisition was achieved using in-house LabVIEW (National Instruments) software. The group velocity dispersion of the probing pulse was determined using nonresonant optical Kerr effect (OKE) measurements. Sample solutions were adjusted to show absorbance of 1.0 at the excitation wavelength.

RESULTS AND DISCUSSION

Design and Synthesis of the Dyads. The 2,6-diiodobodipy part in the dyads is responsible for the production of triplet excited state (Scheme 1). The styrylbodipy part is the singlet energy acceptor for the FRET. Given that the ISC was completely quenched by the FRET effect, and the charge transfer state (CTS) does not lead to formation of the T_1 state of the styrylbodipy moiety, then no triplet state will be produced by **B-1**.[47] In order to attain acid-switchable triplet state production, electron donating moiety dimethylamino styrylbodipy unit was used in **B-2**,[47] which is able to be protonated by acid, thus the singlet and triplet state property of the compounds can be tuned by acid/base. The preparation of the compounds is based on the routine methods for the bodipy chromophore (Scheme 1). The 2,6-diiodobodipy and the styrylbodipy parts are connected by the Cu(I) catalyzed Click reaction. All the compounds were obtained with moderate-to-satisfactory yields.

UV−vis Absorption and Photoluminescence Spectroscopy. The UV−vis absorption spectroscopies of the compounds were studied (Figure 2 and Table 1). The energy donor 2,6-diiodobodipy (compound **9**) gives strong absorption at 538 nm, while compound **10**, a reference compound of singlet energy acceptor, gives intense absorption at 628 nm

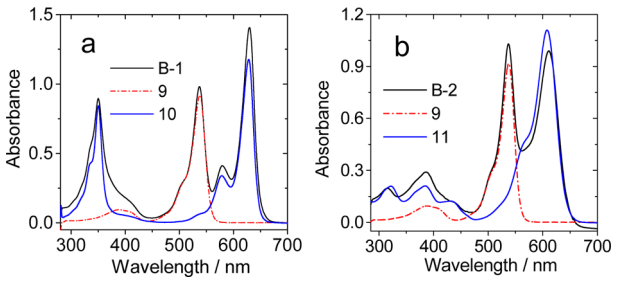

Figure 2. UV−vis absorption spectra of (a) **B-1**, **9**, and **10**; (b) **B-2**, **9**, and **11**. c = 1.0 × 10^{-5} M in toluene, 20 °C.

DOI: 10.1021/acs.jpca.5b03463
J. Phys. Chem. A 2015, 119, 6791−6806

Table 1. Photophysical Parameters of the Compounds

	λ_{abs} (nm[a])	ε[b]	λ_{em} (nm[c])	Φ_L[d]	τ_T (μs[e])	τ_F (ns[f])	Φ_Δ[g]
B-1	630/537	1.41/0.98	643	69.0%	385	4.65	0.35[i]/0.19[k]
9	538	0.92	556	3.6%[h]	133	0.19	0.85[k]
10	628	1.18	641	59.0%[h]	–[l]	4.92	–[l]
B-2	538/612	1.03/0.99	649	26.4%	234	2.50	–[l]
11	608	1.10	645	26.0%	–[l]	3.90	–[l]
B-2+TFA	538/563	1.17[m]/1.23[m]	574	13.8%	165	2.35	0.45[k]
B-3	504/629	0.85/1.22	641	63.0%	–[l]	4.76	–[l]
12	503	0.88	515	90.0%[h]	–[l]	3.44	–[l]

[a]Maximal UV/vis absorption wavelength in toluene (1.0×10^{-5} M). [b]Molar absorption coefficient at absorption maxima. ε: 10^5 M^{-1} cm^{-1}. [c]Maximal emission wavelength in toluene (1.0×10^{-5} M). [d]The fluorescence quantum yields in toluene, with **10** as the standard (Φ_L = 59.0%, in toluene). [e]Measured by transient absorption in toluene (1.0×10^{-5} M), λ_{ex} = 536 nm. [f]The fluorescence lifetime, in toluene (1.0×10^{-5} M). [g]Singlet oxygen quantum yields in DCM. For the absorption peak with shorter wavelength, Rose Bengal (Φ_Δ = 0.8 in MeOH) and diiodo-Bodipy were used as standard (Φ_Δ = 0.87 in DCM). For the absorption peak with longer wavelength, methylene blue (Φ_Δ = 0.57 in DCM) and **B** as standard (Φ_Δ = 0.89 in DCM). [h]Literature values.[24,44] [i]λ_{ex} = 635 nm. [k]λ_{ex} = 530 nm. [l]Not applicable. [m]In the presence of 500 equiv of TFA.

(Figure 2a). Note these monochromophore-based compounds give only one major absorption band in the visible spectral region, this is also the typical feature of the conventional triplet PSs.[7,12−14,55−57] For dyad **B-1**, however, two strong absorption bands in the visible spectral region were observed at 538 and 628 nm, respectively (Figure 2a). The absorption spectrum of **B-1** is the sum of compounds **9** and **10**. Thus, there is no significant interaction between the chromophores in **B-1** at ground state.[38−43,50,58,59] Similar results were observed for dyad **B-2**, and the reference **9** and **11** (Figure 2b). Broadband absorption spectrum was observed for the heavy atom-free reference compound **B-3** (Figure S25 of the Supporting Information). The spectral separation of the energy donor and acceptor in **B-1** and **B-2** are larger than a previously reported diiodobodipy-rhodamine dyad[51] and a diiodobodipy-perylenebisimide (PBI) dyad and triad,[52] which may be helpful for assignment of the time-resolved transient absorption spectra.

No significant changes were observed for the UV−vis absorption spectra of the dyads in solvents with different polarity (see Figure S26 of the Supporting Information), therefore, no interaction, such as electron transfer or $\pi-\pi$ stacking, exists for the dyads at the ground state. These results indicate that intramolecular electron transfer, if there is any, will occur only at the excited state.

The fluorescence spectra of the compounds were studied with optical density matched solutions (Figure 3). The emission of compound **9** is centered at 550 nm (see Figure S28 of the Supporting Information), the overlap of this emission band with the absorption of styrylbodipy unit in **B-1** ensures FRET. The styrylbodipy unit in **B-1** gives a much red-shifted emission band at 650 nm (Figure 3a). The solvent polarity-dependency of the fluorescence spectra was studied. For **9**, the fluorescence emission decreases slightly with increasing of the solvent polarity (from toluene to methanol and acetonitrile. See Figure S28 of the Supporting Information). For compound **10**, blue shifting of the emission band with increasing the solvent polarity was observed (Figure 3b). Moreover, the emission intensity was increased in polar solvents such as acetonitrile as compared with that in toluene. For dyad **B-1** (Figure 3a), however, more significant polarity-dependent emission was observed as compared with that of compound **10**, although the emission of **B-1** can be assigned to the emission from the styrylbodipy unit. The fluorescence emission decreases significantly with increasing of the solvent polarity. For example, the fluorescence intensity of compound **B-1** in toluene is 2.5-fold of that in CH_3CN or methanol (Figure 3a). Quenching of the emission in polar solvents for **B-1** indicates photoinduced electron transfer (PET) in **B-1**.[49,61] However, the PET process is not so efficient as the NDI triad system that we studied previously (no fluorescence can be observed in polar solvents such as CH_2Cl_2 for NDI triad).[53]

The solvent polarity-dependency of the emission of **B-2** and the reference compound **11** was also studied (Figure 4). Compound **11** shows a highly solvent polarity-dependent emission, the fluorescence was significantly quenched in polar solvents (Figure 4b). This is due to the intramolecular charge transfer character of the dimethylaminostyrylbodipy moiety.[62] **B-2** shows similar emission property.

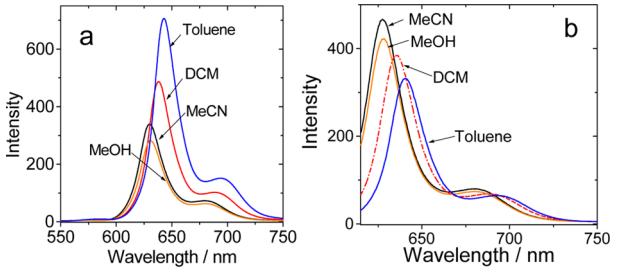

Figure 3. Fluorescence emission spectra of (a) **B-1** (λ_{ex} = 517 nm); (b) **10** (λ_{ex} = 605 nm). Optically matched solutions were used (the solutions in each figure show the same absorbance at the excitation wavelength, c = ca. 1.0×10^{-5} M). 20 °C.

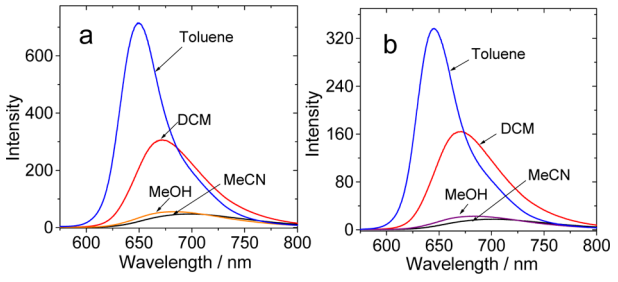

Figure 4. Fluorescence emission spectra of (a) **B-2** (λ_{ex} = 508 nm); (b) **11** (λ_{ex} = 555 nm) in different solvents. The absorbance of the solutions at the excitation wavelength is the same (optically matched solution), 20 °C.

DOI: 10.1021/acs.jpca.5b03463
J. Phys. Chem. A 2015, 119, 6791−6806

The RET in **B-1** and **B-2** was studied by comparison of the fluorescence emission of the energy donor with the dyad (Figure 5). For **B-1**, the emission of the energy donor part

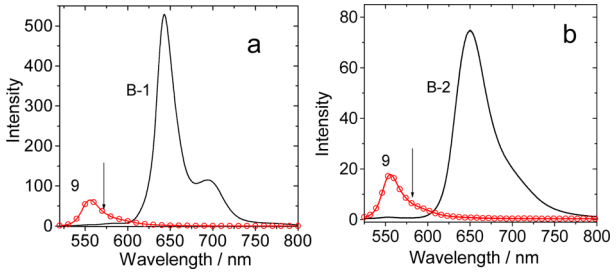

Figure 5. Comparison of the fluorescence emission spectra of the energy donor and the dyads. Fluorescence emission spectra of (a) **B-1** and **9** (λ_{ex} = 510 nm) and (b) **B-2** and **9** (λ_{ex} = 508 nm). Optically matched solutions were used. c = ca. 1.0 × 10^{-5} M in toluene, 20 °C.

(reference compound **9**) was completely quenched (Figure 5a). This quenching effect indicated efficient FRET from the diiodobodipy unit to the styrylbodipy unit, although ET cannot be excluded (see later section) because the emission of the styrylbodipy in **B-1** is more sensitive to the solvent polarity than the reference emitter (compound **10**), which is probably an indication of PET.[50,59,63,64] Similar quenching effect of the diiodobodipy part in **B-2** was observed (Figure 5b). Quenching of the fluorescence of the donor was observed for **B-3** (Figure S30 of the Supporting Information).

The FRET in **B-1** and **B-2** was also confirmed by comparison of the emission of the energy acceptor and **B-1** upon selective photoexcitation into the energy donor (2,6-diiodobodipy) (Figure 6). Given that FRET occurred, the emission of **B-1**

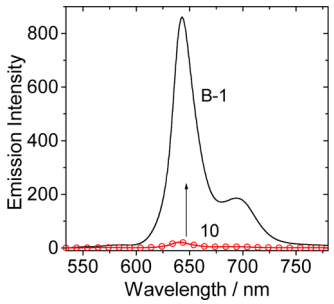

Figure 6. Fluorescence emission spectra of **B-1** and **10** upon excitation into the energy donor. λ_{ex} = 524 nm. c = 1.0 × 10^{-5} M in toluene, 20 °C.

will be enhanced as compared with the reference **10**, upon selective photoexcitation into the energy donor in **B-1**. Indeed the emission of **B-1** is enhanced as compared with that of **10** upon excitation at 524 nm (Figure 6). The emission of **B-1** should not be enhanced without FRET; even **B-1** shows intense absorption at 524 nm as compared with that of compound **10**. Thus, FRET effect in **B-1** is confirmed. Similar results were observed in solvent CH_3CN (see Figure S32 of the Supporting Information). Interestingly, the emission intensity enhancement in toluene (44-fold) is more significant than that in acetonitrile (10-fold), indicating that electron transfer quenching effect is more significant in CH_3CN.

Similar results were also observed for **B-3** (see Figure S35 of the Supporting Information). For **B-2** and compound **11** (see Figure S34 of the Supporting Information), the enhancement is much weaker than that of **B-1**/**10** (probably due to the more significant PET in **B-2**, see later section). The important conclusion drawn from these data is that the ISC in **B-1** is substantially inhibited by the FRET, otherwise no enhancement of the fluorescence emission of the energy acceptor can be observed (Figure 6).

In order to confirm the RET in the dyads, the fluorescence excitation spectra of the dyads were compared with the UV−vis absorption spectra (Figure 7).[43] Two bands were observed for

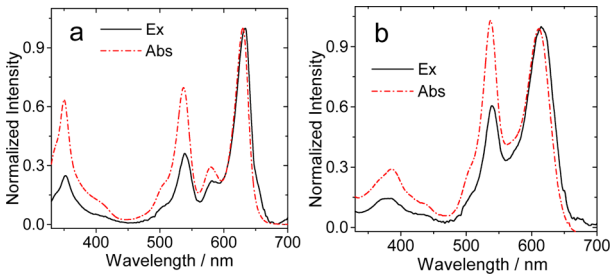

Figure 7. Comparison of the fluorescence excitation spectra and the UV−vis absorption spectra of (a) **B-1** (λ_{em} = 650 nm) and (b) **B-2** (λ_{em} = 650 nm). UV−vis absorption spectra were measured at c = 1.0 × 10^{-5} M and fluorescence excitation spectra were measured at c = 1.0 × 10^{-6} M. In toluene, 20 °C.

B-1 and **B-2** with the emission of the styrylbodipy part set as the emission wavelength for the measurement of the excitation spectra, thus efficient RET in these dyads were confirmed. These results also indicated that the ISC of the spin converters in **B-1** and **B-2** will be substantially inhibited by FRET. Given the ISC is much faster than the FRET process, the band at shorter wavelength will be much weaker in the fluorescence excitation spectra.

The electron transfer process (with styrylbodipy as the electron donor and diiodobodipy part as the electron acceptor) was studied by the comparison of the fluorescence emission of the energy acceptor in **B-1** with **10** (Figure 8). The emission

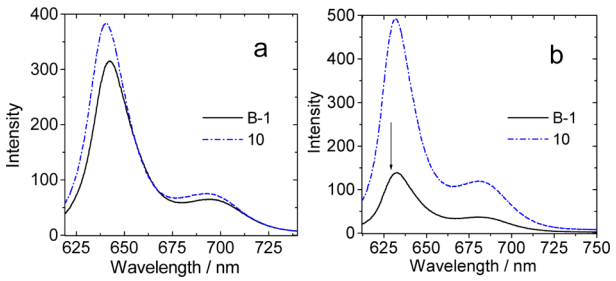

Figure 8. Fluorescence emission spectra of **B-1** and **10** in (a) toluene (λ_{ex} = 609 nm) and (b) CH_3CN (λ_{ex} = 602 nm). Optically matched solution were used. The absorbance of the solution at the excitation wavelength in each figure is the same. 20 °C.

intensity of **B-1** in toluene is similar to that of compound **10** (Figure 8a). This property is drastically different from our previous study on a diiodobodipy-perylenebisimide (PBI) triad, for which the fluorescence of the energy acceptor was completely quenched due to the PET effect, even in the nonpolar solvent such as toluene.[52]

In polar solvent acetonitrile, however, the emission of **B-1** is much weaker than that of compound **10** (Figure 8b). This

DOI: 10.1021/acs.jpca.5b03463
J. Phys. Chem. A 2015, 119, 6791−6806

quenching effect in polar solvent is probably due to the photoinduced electron transfer.[11] The rate constant of the postulated electron transfer process can be calculated by the fluorescence quantum yields of compound **10** and **B-1** according to eq 1,[61] where $\Phi_{(10)}$ is the fluorescence quantum yield of compound **10**, $\Phi_{(B\text{-}1)}$ is the fluorescence quantum yield of compound **B-1**, τ is the fluorescence lifetime of compound **10**.

$$k_{CS}^{intra} = \left[\frac{\Phi_{(10)}}{\Phi_{(B-1)}}\right]/\tau_{(10)} \quad (1)$$

The rate constants of the postulated electron transfer of different solvents of toluene, dichloromethane, CH_3CN, and MeOH were calculated as $k_{CS} = 2.4 \times 10^8$ s^{-1}, 3.5×10^8 s^{-1}, 6.3×10^8 s^{-1}, and 6.9×10^8 s^{-1}, respectively.

The fluorescence lifetimes of compound **10** and **B-1** in different solvents were measured (Table 2). In toluene, compounds **10** and **B-1** give similar fluorescence lifetimes of 4.92 and 4.65 ns, respectively. With increasing of the solvent polarity, the fluorescence lifetime of **B-1** decreased to 2.24 ns in acetonitrile (Table 2).

Table 2. Luminescence Lifetimes of B-1 and 10 in Different Solvents (ns)[a]

	toluene[b]	CH_2Cl_2[c]	CH_3CN[d]	MeOH[e]
B-1	4.65	3.60	2.24	2.58
10	4.92	5.14	5.30	4.98

[a] $c = 1.0 \times 10^{-5}$ M in different solvents at 20 °C. λ_{ex} = 405 nm. [b] λ_{em} = 630 nm. [c] λ_{em} = 638 nm. [d] λ_{em} = 630 nm. [e] λ_{em} = 643 nm.

Acid-Switching of the UV−vis Absorption and Fluorescence Emission of B-2. The dimethylaminostyryl moiety in **B-2** can be protonated with strong acid, such as trifluoroacetic acid (TFA). Thus, the effect of protonation of the dimethylamino group on the UV−vis absorption and fluorescence emission of **B-2** and **11** were studied (Figure 9). Upon addition of TFA, the absorption band at 612 nm decreased (Figure 9a), concomitantly a new absorption band at 562 nm emerged. An isosbestic point at 572 nm was observed. The absorption band at 562 nm is attributed to the protonated dimethylaminostyryl bodipy unit, which is supported by the corresponding spectral changes of reference compound **11** (Figure 9c).[62,65] The absorption band at 537 nm, which is due to the diiodobodipy unit, does not change significantly upon addition of TFA (Figure 9a).

The fluorescence emission of **B-2** in the presence of TFA was also recorded (Figure 9b, excitation into the energy donor). Upon addition of TFA, the emission band of **B-2** at 650 nm decreased and a new emission band at 574 nm developed. This new emission band is due to the protonated dimethylaminostyrylbodipy part, which is supported by the UV−vis absorption and fluorescence emission spectra of the protonated compound **11** (Figure 9, panels c and d). On the basis of the absorption and fluorescence emission wavelength, we conclude that the dimethylaminostyrylbodipy part is the FRET energy acceptor in **B-2**. In the later section, we will show that the triplet state property of **B-2** was changed by addition of TFA.[47] The UV−vis absorption and fluorescence emission changes are more significant than a previously reported diiodobodipy-rhodamine dyad, which is also switchable with acid.[51]

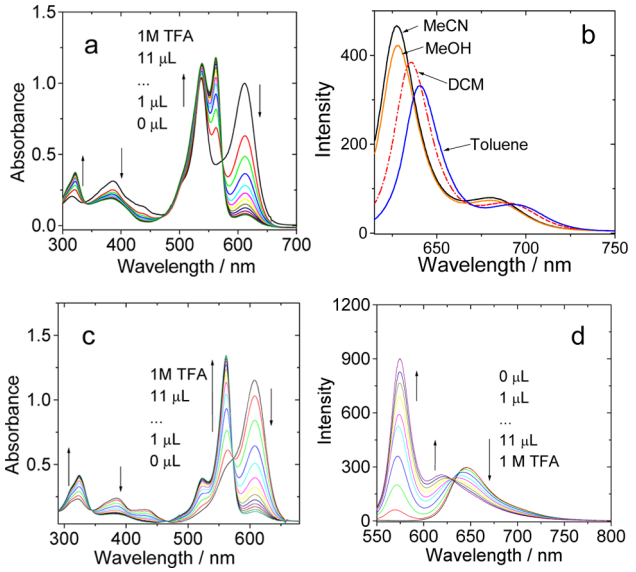

Figure 9. Variation of the UV−vis absorption and the fluorescence spectra upon addition of trifluoroacetic acid (TFA). (a) **B-2** with increasing amount of 1 M TFA was added and (b) the corresponding change of the emission spectra (λ_{ex} = 512 nm). (c) **11** with increasing amount of 1 M TFA was added and (d) the corresponding change of the emission spectra (λ_{ex} = 470 nm). The aliquots of the TFA (1 M in DCM) added are 1, 2, 3, 4, 5, 6, 7, 8, 9, 10, and 11 μL. $c = 1.0 \times 10^{-5}$ M in toluene. 20 °C.

Electrochemical Studies: Cyclic Voltammetry. Electrochemical data of the compounds are useful for determination of the Gibbs free energy changes (ΔG_{CS}^0) of the electron transfer, as well as the energy level of the charge transfer state (CTS), thus it is crucial for elucidation of the photophysical property of the compounds.[49,50] The cyclic voltammetry (CV) of the compounds was determined (Figure 10). For compound **9**, reversible oxidation and reduction waves at +1.53 and −0.81 V were observed (Figure 10a). For styrylbodipy, reversible oxidation wave at +1.12 V was observed, indicating that styrylbodipy is able to be oxidized more easily compared with diiodobodipy (Figure 10a). Thus, styrylbodipy part in **B-1** is more likely to be an electron donor than the diiodobodipy.

For **B-1**, two irreversible oxidation waves at +1.14 V and +1.55 V were observed (Figure 10c). A reversible reduction wave at −0.81 V was observed. Since the redox waves of **B-1** is the sum of **9** and **10**, thus we postulate that the interaction between the components in **B-1** is negligible at ground state.[49] **11** gives two reversible oxidation waves at +0.81 V and +1.13 V (Figure 10b), respectively. This result indicates that the dimethylaminostyrylbodipy is more easily oxidized as compared with that of **9**. A reduction band at −0.97 V was observed. **B-2** shows two reversible reduction waves at −0.81 and −0.96 V, respectively (Figure 11d). No reversible oxidation bands were observed for **B-2**. The main redox potentials of the compounds were summarized in Table 3.[50]

The Gibbs free-energy changes for the electron transfer of the dyads **B-1**, **B-2**, and **B-3** were calculated with the equation of 2:

DOI: 10.1021/acs.jpca.5b03463
J. Phys. Chem. A 2015, 119, 6791−6806

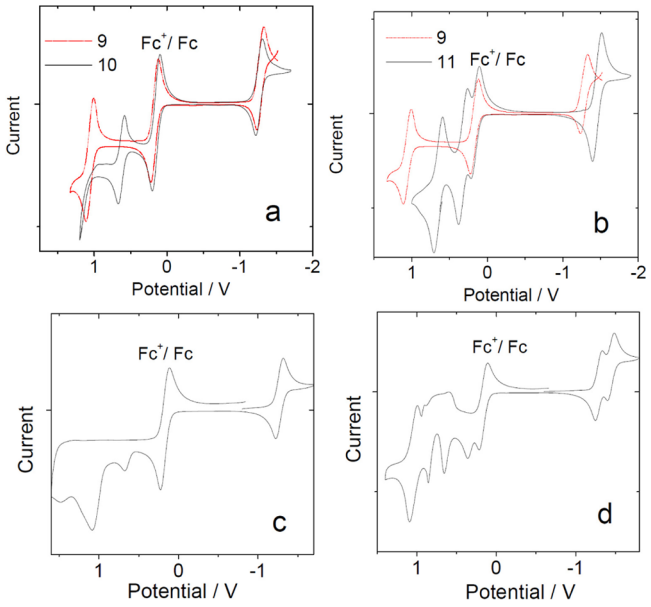

Figure 10. Cyclic voltammogram of **B-1**, **B-2**, and refs **9**, **10**, and **11**. Ferrocene (Fc) was used as the internal reference [$E_{1/2}$ = +0.64 V (Fc^+/Fc) vs standard hydrogen electrode]. (a) **9** and **10**, (b) **9** and **11**, (c) dyad **B-1** and Fc, (d) dyad **B-2** and Fc. In deaerated DCM solutions containing 1.0 mM photosensitizers alone, or with ferrocene, 0.10 M Bu_4NPF_6 as supporting electrolyte, $Ag/AgNO_3$ reference electrode, scan rates: 0.1 V/s. 20 °C.

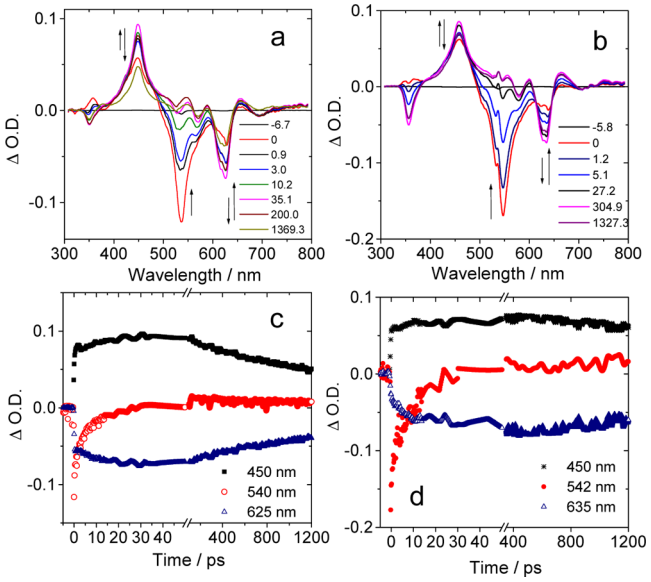

Figure 11. Femtosecond time-resolved transient absorption spectra of **B-1** in (a) CH_3CN and (b) toluene. λ_{ex} = 530 nm. The decay curves at a few selected wavelengths were presented in (c and d, respectively). c = 1.0 × 10^{-5} M. 20 °C.

$$\Delta G^0_{CS} = e[E_{ox} - E_{RED}] - E_{00} - \frac{e^2}{4\pi\varepsilon_0\varepsilon_S R_{CC}} - \frac{e^2}{8\pi\varepsilon_0}\left(\frac{1}{R_D} + \frac{1}{R_A}\right)\left(\frac{1}{\varepsilon_{REF}} - \frac{1}{\varepsilon_S}\right) \quad (2)$$

$$-\Delta G_{CR} = e[E_{OX} - E_{RED}] + \Delta G_S \quad (3)$$

$$\Delta G_S = -\frac{e^2}{4\pi\varepsilon_0\varepsilon_S R_{CC}} - \frac{e^2}{8\pi\varepsilon_0}\left(\frac{1}{R_D} + \frac{1}{R_A}\right)\left(\frac{1}{\varepsilon_{REF}} - \frac{1}{\varepsilon_S}\right) \quad (4)$$

where ΔG_S is the static Coulombic energy, which is described by eq 4, e = electronic charge, E_{OX} = half-wave potential for one-electron oxidation of the electron-donor unit, E_{RED} = halfwave potential for one-electron reduction of the electron-acceptor unit; note herein the anodic and cathodic peak potentials were used because in some cases the oxidation is irreversible, therefore the formal potential $E_{1/2}$ cannot be derived; $E_{0,0}$ is the energy level approximated with the fluorescence emission wavelength (for the singlet excited state), or 1.65 eV for the T_1 state energy of diiodobodipy. ε_S = static dielectric constant of the solvent, R_{CC} = (18.0 Å for **B-1** and 16.0 Å for **B-2**) center-to-center separation distance determined by DFT optimization of the geometry, R_D is the radius of the BODIPY-based donor, R_A is the radius of the electron acceptor, ε_{REF} is the static dielectric constant of the solvent used for the electrochemical studies, and ε_0 permittivity of free space. The solvents used in the calculation of free energy of the electron transfer is dichloromethane (ε = 8.9).

On the basis of the redox potentials of the compounds, electron transfer for **B-1** and **B-3** in toluene is endoenergetic [i.e., no photoinduced intramolecular electron transfer exists (styrylbodipy as electron donor and bodipy part as the electron acceptor)]. In the polar solvent such as MeCN, however, the electron transfer is exoenergetic, thus photoinduced electron transfer is thermodynamically allowed.[11] These results are in agreement with the experimental results that the fluorescence emission of **B-1** is quenched in polar solvents but not in nonpolar solvents such as toluene. For **B-2**, the driving force for electron transfer is more significant than that of **B-1**. The energy levels of the CTS of **B-1** and **B-2** in different solvents were calculated and will be discussed in the later section.[49] Previously, we prepared diiodobodipy-PBI triads, the PET is more significant,[52] which is different from the dyads reported in this work.

Femtosecond Transient Absorption Spectroscopy. Femtosecond time-resolved transient absorption spectroscopy of the compounds was studied (Figures 11 and 12),[49,50,64−67] which was not investigated in the NDI-triad system.[53] Upon selective excitation into the diiodobodipy part in the dyad **B-1**, bleaching bands at 535 and 615 nm were observed, which are attributed to the ground state bleaching of the diiodobodipy part and the styrylbodipy part, respectively (Figure 11, panels a and b). On the basis of the optical density (O.D.) values of the two major bleaching bands and the steady-state absorption of **B-1** (Figure 2), we conclude that it was mainly the diiodobodipy unit in **B-1** that was photoexcited. An excited state absorption (ESA) band at 450 nm was observed for **B-1** (Figure 11a), which was most attributed to the $S_1 \rightarrow S_n$ absorption of the styrylbodipy part, supported by the femtosecond transient absorption of the reference compound **10** (see Figure S50 of the Supporting Information). The decay trace at 540 and 625 nm (Figure 11c) indicates that the bleaching band at 540 nm decays within ca. 14.4 ps (k = 6.9 × 10^{10} s^{-1}), in agreement with the increase of the bleaching band at 625 nm (Figure 11c). Therefore, we propose that there is an ultrafast singlet energy transfer (FRET) in **B-1**. The fast energy transfer process is attributed to the good spectral overlap between the emission of the diiodobodipy part and the absorption of the styrylbodipy unit (energy acceptor). It should

DOI: 10.1021/acs.jpca.5b03463
J. Phys. Chem. A 2015, 119, 6791−6806

Table 3. Electrochemical Redox Potentials (V vs Fc/Fc^+) and Driving Forces of Charge Recombination (ΔG_{CR}) and Charge Separation (ΔG_{CS}) for Dyads B-1, B-2, and B-3 via ^{1}(iodo-BDP)* and ^{1}(StyrylBDP)* in Acetonitrile, DCM, and Toluene

	IodoBDP$^{0/\bullet-}$ [V]	styrylBDP$^{0/\bullet+}$ [V]	ΔG_{CR} [eV] ($PhCH_3$)	ΔG_{CS} [eV] ($PhCH_3$)	ΔG_{CR} [eV] (CH_3CN)	ΔG_{CS} [eV] (CH_3CN)	ΔG_{CR} [eV] (CH_2Cl_2)	ΔG_{CS} [eV] (CH_2Cl_2)
9	−0.81	–	–	–	–	–	–	–
10	–	+1.12	–	–	–	–	–	–
11	–	+0.81, +1.13	–	–	–	–	–	–
B-1	−0.81	+1.14	−2.31	+0.08[a] +0.37[b]	−1.74	−0.52[a] −0.23[b]	−1.86	−0.39[a] −0.08[b]
B-2	−0.81	+0.84	−1.92	−0.50[a] −0.18[b]	−1.44	−0.75[a] −0.26[b]	−1.55	−0.70[a] −0.29[b]
B-3	−1.06	+1.16	−2.58	+0.18[c] +0.64[b]	−2.01	−0.39[c] +0.04[b]	−2.13	−0.27[c] +0.19[b]
12	−1.06	–	–	–	–	–	–	–

[a]Via ^{1}[iodoBDP]*. [b]Via ^{1}[StyrylBDP]*. [c]Via ^{1}[BDP]*.

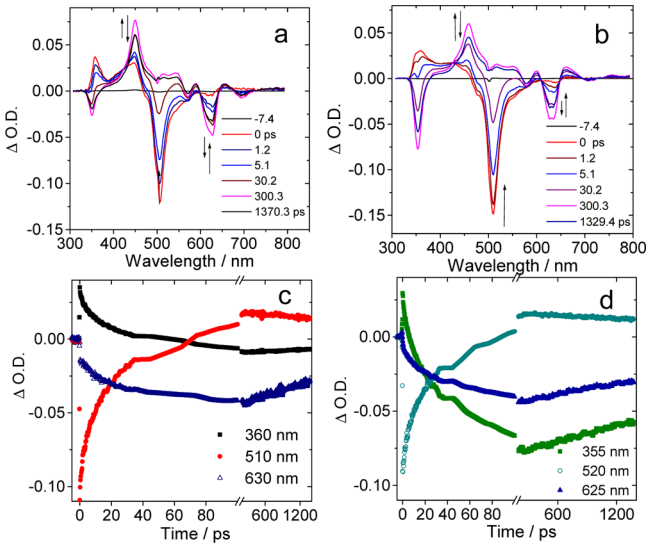

Figure 12. Femtosecond time-resolved transient absorption spectra of **B-3** in (a) CH_3CN and (b) in toluene. λ_{ex} = 500 nm. The decay curves at a few selected wavelengths were presented in (c and d, respectively). $c = 1.0 \times 10^{-5}$ M. 20 °C.

be noted that there is no significant population of the triplet excited state of the styrylbodipy unit, indicated by the TA spectra of **B-1** and our previous study of the triplet excited state of styrylbodipy unit with nanosecond transient absorption spectroscopy.[25] These results indicate that the ultrafast singlet energy transfer in **B-1** out-competed the ISC of the diiodobodipy unit, which takes about 100 ps (see Figure S51 of the Supporting Information).[68] These postulations are in agreement with the low triplet state yield (Φ_T = 36%) of **B-1** as compared to that of compound **9** (Φ_T = 84%). Similar results were observed for **B-2** (Φ_T = 57%; Figure S52 of Supporting Information). We noted that no triplet state of the diiodobodipy was observed in the femtosecond transient absorption spectra, which may be due to the fast TTET process (can be up to 5 ps).[69] As a result, the population of the diiodobodipy triplet state is negligible at all times.

Previously, we studied diiodobodipy-perylenebisimide (PBI) dyad and triad, which are with competitive ISC and FRET, but the ISC was not inhibited by FRET, and high singlet oxygen yields were observed for those dyad (Φ_Δ = 80%) and triad (Φ_Δ = 78%).[52] For **B-1**, however, the ISC was greatly inhibited by the FRET.

The femtosecond transient absorption spectra of the reference compound **B-3** were also studied (Figure 12). Upon femtosecond pulsed laser excitation at 500 nm, the ground state bleaching bands at 510 and 620 nm were observed, which are attributed to the bodipy moiety and the styrylbodipy moiety, respectively. The ESA bands at 450 nm are attributed to the $S_1 \rightarrow S_n$ transitions of the styrylbodipy part.

By monitoring the decay traces at a few critical wavelengths, we propose there exist FRET for **B-3**. For example, the bleaching band at 500 nm decay within ca. 40.3 ps, at the same time, the bleaching band at 615 nm is enhanced. The rate constant of the FRET was calculated as $k_{FRET} = 2.5 \times 10^{10}$ s^{-1}, based on the fitting of the decay curves (Figure 12, panels c and d). These results indicate that the singlet energy transfer in **B-3** is much slower than that of **B-1**.

Nanosecond Transient Absorption Spectroscopy. Nanosecond time-resolved transient absorption spectra of the dyads were investigated to study the triplet excited states (Figure 13).[70] For **B-1**, bleaching band at 623 nm was observed

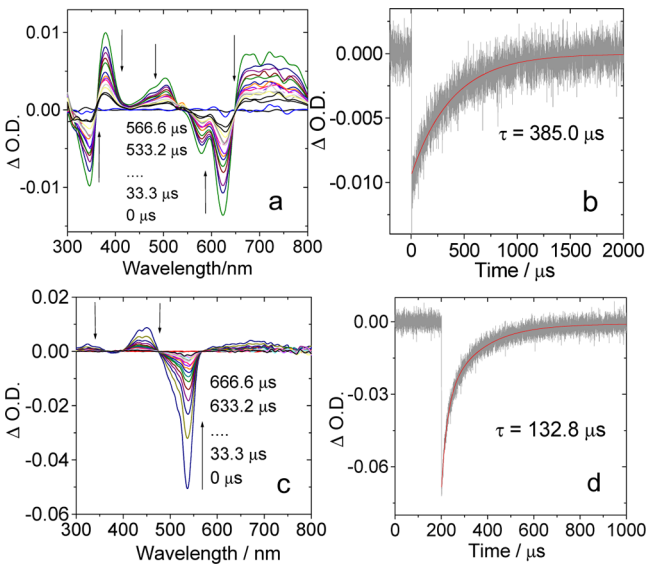

Figure 13. Nanosecond time-resolved transient absorption spectra of **B-1** and compound **9**. (a) **B-1** upon pulsed laser excitation (λ_{ex} = 536 nm) and (b) decay trace of **B-1** at 630 nm. (c) **9** upon pulsed laser excitation (λ_{ex} = 536 nm) and (d) decay trace of **9** at 530 nm. $c = 1.0 \times 10^{-5}$ M in deaerated toluene, 20 °C.

DOI: 10.1021/acs.jpca.5b03463
J. Phys. Chem. A 2015, 119, 6791−6806

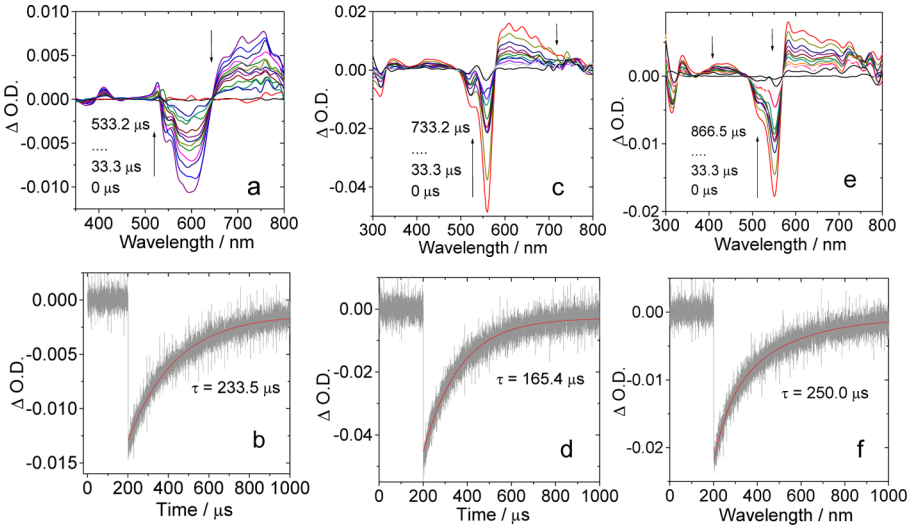

Figure 14. Effect of protonation with TFA and the solvent polarity on the triplet state property of **B-2**. (a) Nanosecond transient absorption spectra of **B-2** upon pulsed laser excitation and (b) decay traces of **B-2** at 560 nm, $c = 1.0 \times 10^{-5}$ M in toluene. (c) Transient absorption spectra of **B-2** in the presence of TFA (11 μL) and (d) decay trace of **B-2** in the presence of TFA (11 μL) at 560 nm. $c = 1.0 \times 10^{-5}$ M in toluene. (e) Transient absorption spectra of **B-2** in the presence of TFA (11 μL) and (f) decay trace of **B-2** in the presence of TFA (11 μL) at 560 nm. $c = 1.0 \times 10^{-5}$ M in deaerated CH_3CN. All the excitations are at λ_{ex} = 536 nm. 20 °C.

upon selective photoexcitation into the singlet energy donor [i.e., the diiodobodipy unit (Figure 13a)]. The triplet state lifetime was determined as 385.0 μs (Figure 13b). No bleaching band at 530 nm was observed. For compound **9**, strong bleaching band at 538 nm was observed upon 536 nm pulsed laser excitation (Figure 13c), the triplet state lifetime was determined as 132.8 μs (Figure 13d).

The transient absorption of **B-1** are same to the results of the triplet state of styrylbodipy moiety observed previously with a styrylbodipy-C_{60} dyad.[25] Population of the triplet excited state of styrylbodipy (Φ_T = 36%) upon selective photoexcitation into the diiodobodipy part (i.e., the singlet/triplet energy donor), indicated triplet energy transfer from the diiodobodipy part to the styrylbodipy part, because the styrylbodipy (compound **10**) alone gives very weak ISC. As a proof of this postulation, no significant production of triplet excited state was observed with **B-3** upon photoexcitation into the energy donor, in which the singlet energy donor is devoid of ISC capability. This finding is different from a previous study on styrylbodipy-iodobodipy molecular logic gates, for which the ISC was believed to be completely inhibited by FRET,[47] because following this explanation, no triplet state should be observed with **B-1**. The intramolecular triplet energy transfer is too fast to be monitored by the nanosecond transient absorption spectrometer (time resolution is 10 ns), thus the rate constant of the triplet state energy transfer $k_{TT} \gg 10^8$ s^{-1}.[67] Photoexcitation into the styrylbodipy part (630 nm) did not produce any long-lived transient species detectable by the nanosecond transient absorption spectrometer. Production of the T_1 state of the styrylbodipy part by charge recombination (CR) is ruled out because CTS is not formed for **B-1** in toluene (confirmed by the electrochemical study and the fluorescence quenching studies). Further support is from **B-3**, which shows no triplet formation upon photoexcitation. The assignment of the localization of the triplet state in **B-1** is more straightforward than a previously studied diiodobodipy-rhodamine dyad and diiodobodipy-PBI dyad and triad, for which the steady state absorption of the two chromophores overlaps.[51,52]

The transient spectra of **B-1** in polar solvents such as CH_2Cl_2 and CH_3CN were also recorded (see Figure S37 of the Supporting Information). The ΔO.D. values of the spectra are much smaller than that in toluene, indicating that the production of the triplet state of styrylbodipy in **B-1** is less efficient in polar solvents, which may be due to the PET process.[11] These results are much different from the naphthalenediimide triad system reported previously, where the triplet state was completely quenched in polar solvents.[53]

Notably, the lifetime of the triplet state of the styrylbodipy part is exceptionally longer (385.0 μs at $c = 1.0 \times 10^{-5}$ M) than the reported NDI-triad (276 μs at $c = 1.0 \times 10^{-5}$ M) and the bodipy-PBI triad (150 μs at $c = 1.0 \times 10^{-5}$ M).[52,53] On the other hand, with iodination of the styrylbodipy (i.e., to access the triplet state via the heavy atom effect), instead the intramolecular sensitizing method in **B-1**, the triplet state lifetime of the same chromophore is much shorter (1.8 μs).[31] The reduced triplet state lifetime in the 2,6-diiodostyrylbodipy may be due to the heavy atom effect of iodine, with which the $T_1 \rightarrow S_0$ can be accelerated. As a result, the triplet state lifetime was reduced. On the contrary, the sensitized production of the triplet excited state of the styrylbodipy moiety in **B-1**, and also in a previously reported styrylbodipy-C_{60} dyad,[25] resulted in a long-lived triplet excited state. Therefore, we propose to use the triplet sensitization, rather than the conventional heavy atom effect,[14] to reveal the inherent triplet state property of organic chromophores which are devoid of the ISC capability.[15]

The nanosecond transient absorption spectra of **B-2** were also studied (Figure 14). Upon pulsed excitation into the diiodobodipy part, no bleaching band at 530 nm was observed (Figure 14a) in toluene. Instead, a bleaching band of the styrylbodipy unit at 600 nm appeared instantly. The triplet state lifetime was determined as 233.5 μs (Figure 14b). Thus, the lack of the triplet state of diiodobodipy moiety in **B-2** indicated efficient intramolecular triplet energy transfer. Previously, the triplet state lifetime of the dimethylaminostyrylbodipy was determined as 4.0 μs with the heavy atom effect (iodination).[20] Interestingly, a very weak production of the triplet state of the styrylbodipy part in **B-2** can be observed upon photoexcitation

DOI: 10.1021/acs.jpca.5b03463
J. Phys. Chem. A 2015, 119, 6791−6806

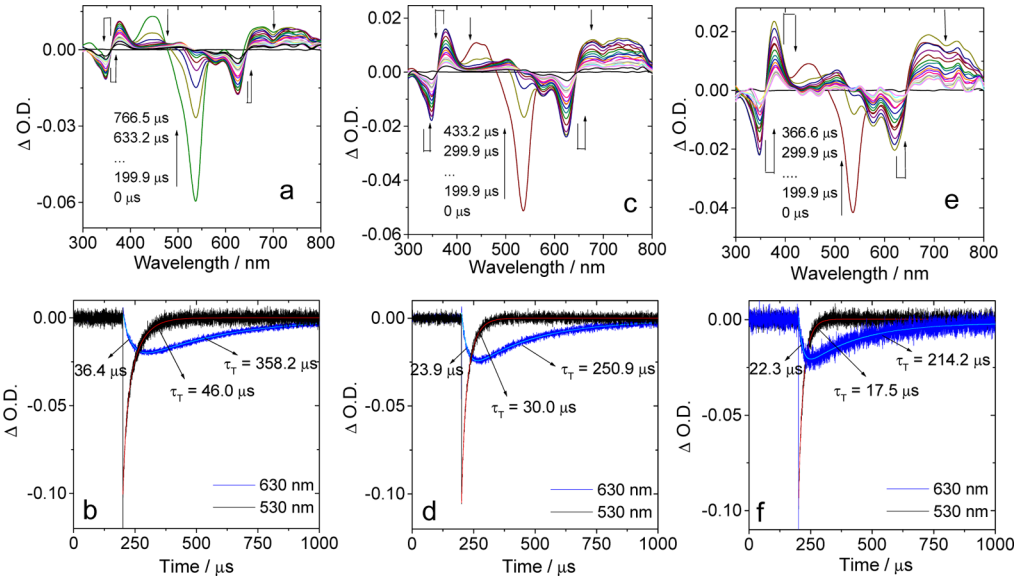

Figure 15. Intermolecular triplet−triplet energy transfer (TTET) from **9** to **10**, monitored by nanosecond transient absorption spectra of the mixture of **9** and **10**. The concentration of compound **9** was fixed at $c = 1.0 \times 10^{-5}$ M, and the molar ratio of **9**:**10** was varied at (a) 1:0.33 and (b) decay trace of the mixture; (c) 1:0.66 and (d) decay trace of the mixture; (e) 1.0:1.0 and (f) the decay trace of the mixture. The decay traces were monitored at 530 and 630 nm, respectively. The energy donor (compound **9**) was selectively excited with OPO pulsed laser at 536 nm (note excitation of compound **10** alone will not give triplet excited state). In deaerated toluene. 20 °C.

at 608 nm (in toluene). Photoexcitation of the reference compound **11** at 608 nm did not produce any triplet state signal. Thus, we propose that the T_1 state of the dimethylaminostyrylbodipy part can be produced by the charge recombination (CR).[49,71] This method may become an alternative to the conventional ways to access triplet state, such as with heavy atom effect of Ru(II), Pt(II), Ir(III) and I, etc.

The effect of protonation of the dimethylaminostyrylbodipy moiety on the triplet state property was also studied (Figure 14c), which is not applicable in the previous naphthalenediimide triad (no-acid responsive moiety was used in the triad).[53] Without protonation, a bleaching band at 600 nm was observed in toluene, and the lifetime of the triplet state was 233.5 ms. Upon addition of TFA, a new bleaching band at 560 nm was observed. The lifetime of the triplet state was determined as 165.4 μs. Thus, both the lifetime and the bleaching feature of the triplet state of **B-2** were changed upon protonation. To the best of our knowledge, switching of the triplet state of organic compounds with external stimuli was rarely reported,[7,8,47,48,72,73] and these novel materials will be very useful for application as activatable photodynamic therapeutic reagents[47,73−75] and molecular devices.[47,75] We found that without protonation, no triplet state of **B-2** can be observed in polar solvents such as acetonitrile; upon protonation with TFA, long-lived triplet state of **B-2** can be observed in polar solvent such as acetonitrile (τ = 250.0 μs, Figure 14, panels e and f). This result can be attributed to the diminished electron transfer effect upon protonation. Herein, the triplet state of dyads **B-1** and **B-3** is clearly localized on the singlet energy acceptor (styrylbodipy part), which is different from the previously reported diiodobodipy-rhodamine dyad (triplet state is localized on the singlet energy donor) (i.e., the diiodobodipy part).[51]

Intermolecular Triplet Energy Transfer. Long-distance intermolecular EnT or ET is crucial for photosynthesis,[66] photoredox catalytic organic reactions,[3,5,76] and photodynamic therapeutic reagents.[14,15] Long-range triplet energy transfer with strong visible light chromophores as energy donor/acceptor was rarely studied. On the other hand, triplet energy acceptor is also important in fundamental photochemistry, such as for determination of triplet state energy levels of chromophores.[73] Conventionally, the triplet energy acceptors are carotene, anthracene, etc.[77−79] Very few new and robust triplet energy acceptors were reported.

Herein, the intermolecular triplet energy transfer was studied with nanosecond transient absorption spectroscopy, with compound **9** as the triplet photosensitizer and compound **10** as the triplet energy acceptor (Figure 15).[80] **9** shows bleaching band at 530 nm upon pulsed laser excitation, indicating the population of the triplet state of diiodobodipy upon photoexcitation. In the presence of compound **10**, a new bleaching band at 625 nm was developed upon pulsed laser excitation of the mixture (Figure 15a). With an elapse of time after the laser flash, the transient absorption feature of the diiodobodipy disappeared gradually, and the final transient spectra is the exact same as that of compound **10** (Figure 15a). Thus, we conclude that intermolecular triplet energy transfer occurs for the mixture of compounds **9** and **10**. It should be pointed out that the production of the triplet state of compound **10** is unlikely due to the intermolecular charge recombination because this intermolecular process is highly endoenergetic in toluene. On the basis of the electrochemical and spectroscopic data, the free energy changes (ΔG) of the intermolecular electron transfer is calculated with the Weller equation as +0.70 eV (see Supporting Information).

The kinetics of the intermolecular triplet state energy transfer were studied by monitoring the decay traces at specific wavelengths (Figure 15, panels b, d, and f). The lifetime of the triplet state of diiodobodipy was substantially quenched from 132.8 to 46.0 μs in the presence of triplet energy acceptor compound **10** (1:0.33 molar ratio).

Interestingly, the decay trace at 630 nm is biphasic, that is, there is an initial increase of the bleaching band, and then the

DOI: 10.1021/acs.jpca.5b03463
J. Phys. Chem. A 2015, 119, 6791−6806

optical density (O.D.) decreases. The first increasing phase is due to the formation and accumulation of the T_1 state of compound **10** via intermolecular triplet EnT, with compound **9** as energy donor (triplet photosensitizer). The second phase is due to the decay of the T_1 state of compound **10**, after the finish of the TTET process. It should be pointed out that the photophysical processes of decay of T_1 state of **9**, the TTET from **9** to **10**, and the decay of the T_1 state of **10**, are all occurring concomitantly.

Previously, we studied the intermolecular triplet state energy transfer between diiodobodipy and PBI.[52] However, the bleaching bands of the energy donor and the acceptor overlap with each other, and as a result, the decay of the triplet state donor and the accumulation of the triplet acceptor is not distinct. The bleaching band of the components of the dyads **B-1** and **B-2** are at a different position, thus the assignment of the two bleaching bands of the transient absorption spectra is without any difficulties, which is improved compared with the previously reported diiodobodipy-PBI triads.[52] Previously, the intermolecular TTET was also studied with the NDI triad.[53]

At higher triplet acceptor concentration, the lifetime of the triplet energy donor was reduced significantly, and the rising of the decay trace at 630 nm becomes faster (Figure 15). The TTET rate constants and the TTET efficiency at different triplet acceptor concentration are listed in Table 4. Similar intermolecular triplet state energy transfer was observed for compounds **9** and **11** (see Figure S42 of the Supporting Information).

Table 4. Kinetics of the Intermolecular Triplet State Energy Transfer between Compounds 9 and 10[a]

molar ratio **9**:**10**[b]	$\tau_{530\ nm}$[c] (μs)	$\tau_{630\ nm}$[d] (μs)	$\tau_{630\ nm}$[e] (μs)	k_{TT} (s^{-1})	Φ_{TT}
9 only	132.8	–	–	–	–
1:0.33	46.0	36.4	358.2	2.5×10^4	89.8%
1:0.66	30.0	23.9	250.9	3.8×10^4	90.5%
1:1.0	22.3	17.5	214.2	5.2×10^4	91.8%
1:1.33	14.5	15.0	160.0	6.0×10^4	90.6%
1:1.66	15.3	15.2	167.7	6.0×10^4	90.9%
10 only	–	–	385.0	–	–

[a]Determined with nanosecond time-resolved transient difference absorption spectroscopy. [b]With compound **9** at 1.0×10^{-5} M in deaerated toluene. [c]Lifetime monitored at 530 nm. Upon pulsed excitation at 536 nm. [d]The lifetime for the first phase of the trace at 630 nm. [e]The lifetime for the second phase of the trace at 630 nm. [f]Triplet–triplet energy transfer rate constant, $k_{TT} = (1/\tau_2) - (1/\tau_1)$. τ_1 is the triplet state lifetime of the triplet energy donor in the absence of energy acceptor; τ_2 is the triplet state lifetime of the triplet energy donor in the presence of energy acceptor. [g]Triplet–triplet energy transfer efficiency. $\Phi_{TT} = 1 - (\tau_2/\tau_1)$.[82]

In consideration of the chromophore, styrylbodipy is with high photostability, strong visible light absorption, low triplet formation quantum yield upon direct photoexcitation, and with the feasible derivatization of the bodipy chromophore, we propose that the bodipy derivatives can be used as a new kind of triplet energy acceptor for various photochemical studies.[81] For example, compound **11** can be used as a quencher for DNA molecular beacons.[79]

The TTET rate constants were calculated using eq 5.[82] The intermolecular triplet state energy transfer rate constants are in the range from 2.5×10^4 s^{-1} to 6.0×10^4 s^{-1}, depending on the triplet acceptor concentration. The bimolecular rate constants (k_q) are ca. 2.5×10^{11} M^{-1} s^{-1} – 4.2×10^6 M^{-1} s^{-1}, which is ca. 50-fold higher than the intermolecular triplet state energy transfer between the zinc phthalocyanine complex and subphthalocyanine.[80] The energy transfer rate constants are ca. 10-fold of the intra-assembly triplet energy transfer in a C_{60}-ferrocene hydrogen-bonded molecular assembly.[82] The intermolecular triplet energy transfer efficiency is in the range of 90%–92%, which are as efficient as those observed for intra-assembly triplet state energy transfer in hydrogen-bonding C_{60}-ferrocene assembly.[82] We attributed the efficient triplet state energy transfer to the long-lived triplet state of the energy donor (compound **9**).

$$k_{ET} = (1/\tau_2) - (1/\tau_1) \quad (5)$$

$$\Phi_{ET} = 1 - \tau_2/\tau_1 \quad (6)$$

The bimolecular quenching efficiency was also studied. Stern–Volmer quenching constants were calculated as $K_{SV} = 5.94 \times 10^5$ M^{-1}. The bimolecular quenching constant was calculated as $k_q = K_{SV}/\tau_0 = 4.5 \times 10^9$ M^{-1} s^{-1}, where τ_0 is the triplet state lifetime of the triplet energy donor (compound **9**, 133 μs). In order to study the quenching efficiency of the triplet state of compound **9** by compound **10**, which is given by $f_Q = k_q/k_0$, where k_0 is the diffusion-controlled bimolecular quenching rating constants, it can be calculated with the Smoluchowski equation (eq 7),[83] D is the sum of the diffusion coefficients of the energy donor (D_f) and quencher (D_q),

$$k_0 = 4\pi RND/1000 = \frac{4\pi N}{1000}(R_f + R_q)(D_f + D_q) \quad (7)$$

N is Avogadro's number, R is the collision radius, the sum of the molecule radii of the energy donor (R_f) and the quencher (R_q). Diffusion coefficients can be obtained from the Stokes–Einstein equation:[68] k is Boltzmann's constant, η is the solvent viscosity, R is the molecule radius.

$$D = kT/6\pi\eta R \quad (8)$$

The molecule radii of the energy donor (**9**) is 5.5 Å, and it is 7.5 Å for the quencher (**10**). In accordance with eq 8, the diffusion coefficients of the energy donor (**9**) is 6.6×10^{-6} cm^2 s^{-1} and quencher (**10**) is 4.9×10^{-6} cm^2 s^{-1} (in toluene at 20 °C). Thus, k_0 was calculated as 1.1×10^{10} M^{-1} s^{-1}. The quenching efficiency is $f_Q = k_q/k_0 = 39.8\%$.

Jablonski Diagram of the Dyads. The photophysical processes of **B-1** were summarized in Scheme 2. Upon selective photoexcitation into the singlet energy donor (i.e., the diiodoBodipy part), competing FRET and ISC processes exist. Considering that the FRET is much faster than the ISC of the diiodobodipy part in **B-1**, the ISC of the diiodobodipy part is inhibited to a large extent. This postulation was supported by the much smaller singlet oxygen quantum yield of **B-1** (Φ_Δ = 19%) as compared to that of compound **9** (Φ_Δ = 85%). This reduction is efficient than the NDI-triad.[53] Triplet state quantum yield (Φ_T) determination also support this conclusion (Φ_T = 36% for **B-1**, Φ_T = 88% for **9**). Population of the triplet state of the diiodobodipy unit will be followed by an intramolecular triplet energy transfer process, which finally leads to the population of the triplet state of the styrylbodipy part. The ISC of the styrylbodipy part is weak, thus the fluorescence of the styrylbodipy part is with high quantum yield (Φ_F = 59.0%; Table 1). Since the charge transfer state (CTS) of **B-1** in toluene is with high energy level (2.31 eV), neither the

DOI: 10.1021/acs.jpca.5b03463
J. Phys. Chem. A 2015, 119, 6791–6806

Scheme 2. Simplified Jablonski Diagram Illustrating the Photophysical Processes in B-1 (a) in Toluene and (b) in CH_3CN

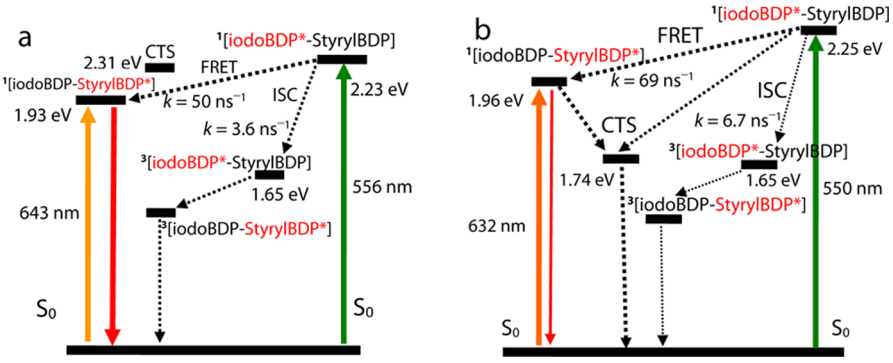

singlet excited state nor the triplet excited states of the dyad **B-1** was affected by the CTS.

The component at the excited state was designated with red color and an asterisk. The number of the superscript designated the spin multiplicity of the excited state. IodoBDP stands for diiodobodipy part, and StyrylBDP stands for styrylbodipy part.

In polar solvents such as acetonitrile, the CTS lies slightly above the triplet state of the diiodobodipy (Scheme 2b). As a result, the fluorescence of the styrylbodipy part will be quenched in acetonitrile as compared to the reference compound **10**. This postulation was confirmed by experimental results (Figure 8). Moreover, the ISC of the diiodobodipy unit is competed by FRET as well as an extra decay channel (i.e., the electron transfer). Thus, the production of the triplet state of diiodobodipy is inhibited in **B-1**. We assume that the charge recombination (CR) process does not produce any triplet state of the styrylbodipy unit significantly.[49] The triplet state quantum yield of **B-1** in toluene and acetonitrile is 36% and 30%, respectively. Similar results were found for **B-2**, the triplet state quantum yields are 57% and 33% in toluene and acetonitrile, respectively.

CONCLUSIONS

In summary, 2,6-diiodobodipy-styrylbodipy dyads were prepared (**B-1** and **B-2**), with the excited state energy levels of the components of the dyads aligned in such a profile that the fluorescence-resonance-energy-transfer (FRET) competes with the intersystem crossing (ISC) of the singlet energy donor. In the dyads, the 2,6-diiodobodipy unit was used as a singlet energy donor and the spin converter for triplet state formation, whereas the styrylbodipy unit was used as singlet energy acceptor, as well as a triplet energy acceptor. With this molecular structural profile, competition between the ISC and FRET is established. The effect of this competing ISC and FRET on the production of triplet excited states was studied with steady state UV−vis absorption and fluorescence spectroscopy, electrochemical analysis, as well as femto-/nanosecond transient absorption spectroscopies. FRET was proved with steady state UV−vis absorption and fluorescence spectra, as well as femtosecond transient absorption spectroscopy. Ultrafast FRET was observed with the iodinated dyad (k_{FRET} = 5.02 × 10^{10} s^{-1}), while the FRET is much slower in an uniodinated reference dyad (**B-3**, k_{FRET} = 1.99 × 10^{10} s^{-1}). The different FRET rate constants were attributed to the different spectral overlap. ISC of the spin converter (2,6-diiodobodipy) was determined as a much slower process (k_{ISC} = 3.60 × 10^9 s^{-1}). Thus, the production of triplet state in the dyad was substantially inhibited as compared with that of 2,6-diiodobodipy. This conclusion was supported by the triplet state formation quantum yields (Φ_T = 36.1% and 57.0% for **B-1** and **B-2**, respectively), as well as the singlet oxygen quantum yields (Φ_Δ = 18.0% and 29.6% for **B-1** and **B-2**, respectively). Intermolecular triplet energy transfer was studied with nanosecond time-resolved transient absorption spectroscopy, which shows efficient TTET (Φ_{TTET} = 91.8%). The TTET kinetics (k_{TTET} = 5.2 × 10^4 s^{-1}) demonstrated that long-lived triplet excited states are ideal for application as triplet photosensitizers for long-range triplet energy transfer. These studies will be useful for designing multichromophore broad-band visible light-absorbing triplet photosensitizers, as well as for study of the fundamental photophysical processes of the multichromophore organic compounds.

ASSOCIATED CONTENT

Supporting Information

Experimental procedures, molecular structure characterization, additional spectra, Stern-Volmer plots, kinetics of the intermolecular triplet state energy transfer, decay trace of the mixture, quantum yield of singlet oxygen, DFT calculations, Jablonski diagrams, molecular orbitals, selected parameters for vertical excitation, and *x*,*y*,*z* coordinates of the compounds. The Supporting Information is available free of charge on the ACS Publications website at DOI: 10.1021/acs.jpca.5b03463.

AUTHOR INFORMATION

Corresponding Authors

*E-mail: zhaojzh@dlut.edu.cn.
*E-mail: kglusac@bgsu.edu.

Author Contributions

§Z.W. and Y.X. contibuted equally to this work.

Notes

The authors declare no competing financial interest.

ACKNOWLEDGMENTS

J.Z. thanks the NSFC (Grants 21273028, 21421005, and 21473020), the Royal Society (U.K.), and NSFC (Cost-Share-21011130154), Ministry of Education (SRFDP-20120041130005), Program for Changjiang Scholars and Innovative Research Team in University [IRT_13R06], State Key Laboratory of Fine Chemicals (KF1203), the Fundamental Research Funds for the Central Universities (DUT14ZD226), and Dalian University of Technology (DUT2013TB07) for financial support. K.D.G. thanks NSF (CHE-1055397) for financial support.

DOI: 10.1021/acs.jpca.5b03463
J. Phys. Chem. A 2015, 119, 6791−6806

REFERENCES

(1) Hari, D. P.; König, B. The Photocatalyzed Meerwein Arylation: Classic Reaction of Aryl Diazonium Salts in a New Light. *Angew. Chem., Int. Ed.* **2013**, *52*, 4734−4743.
(2) Hari, D. P.; König, B. Synthetic Applications of Eosin Y in Photoredox Catalysis. *Chem. Commun.* **2014**, *50*, 6688−6699.
(3) Shi, L.; Xia, W. Photoredox Functionalization of C−H Bonds Adjacent to a Nitrogen Atom. *Chem. Soc. Rev.* **2012**, *41*, 7687−7697.
(4) Ravelli, D.; Fagnoni, M.; Albini, A. Photoorganocatalysis. What for? *Chem. Soc. Rev.* **2013**, *42*, 97−113.
(5) Prier, C. K.; Rankic, D. A.; MacMillan, D. W. C. Visible Light Photoredox Catalysis with Transition Metal Complexes: Applications in Organic Synthesis. *Chem. Rev.* **2013**, *113*, 5322−5363.
(6) Liu, Q.; Li, Y.-N.; Zhang, H.-H.; Chen, B.; Tung, C.-H.; Wu, L.-Z. Reactivity and Mechanistic Insight into Visible-Light-Induced Aerobic Cross-Dehydrogenative Coupling Reaction by Organophotocatalysts. *Chem. - Eur. J.* **2012**, *18*, 620−627.
(7) McDonnell, S. O.; Hall, M. J.; Allen, L. T.; Byrne, A.; Gallagher, W. M.; O'Shea, D. F. Supramolecular Photonic Therapeutic Agents. *J. Am. Chem. Soc.* **2005**, *127*, 16360−16361.
(8) Tian, J.; Ding, L.; Xu, H.-J.; Shen, Z.; Ju, H.; Jia, L.; Bao, L.; Yu, J.-S. Cell-Specific and pH-Activatable Rubyrin-Loaded Nanoparticles for Highly Selective Near-Infrared Photodynamic Therapy against Cancer. *J. Am. Chem. Soc.* **2013**, *135*, 18850−18858.
(9) Schmitt, F.; Freudenreich, J.; Barry, N. P. E.; Juillerat-Jeanneret, L.; Süss-Fink, G.; Therrien, B. Organometallic Cages as Vehicles for Intracellular Release of Photosensitizers. *J. Am. Chem. Soc.* **2012**, *134*, 754−757.
(10) Yukruk, F.; Dogan, A. L.; Canpinar, H.; Guc, D.; Akkaya, E. U. Water-Soluble Green Perylenediimide (PDI) Dyes as Potential Sensitizers for Photodynamic Therapy. *Org. Lett.* **2005**, *7*, 2885−2887.
(11) Novakova, V.; Zimcik, P.; Miletin, M.; Vachova, L.; Kopecky, K.; Lang, K.; Cháberac, P.; Polívka, T. Ultrafast Intramolecular Charge Transfer in Tetrapyrazinoporphyrazines Controls the Quantum Yields of Fluorescence and Singlet Oxygen. *Phys. Chem. Chem. Phys.* **2010**, *12*, 2555−2563.
(12) Awuah, S. G.; You, Y. Boron Dipyrromethene (BODIPY)-Based Photosensitizers for Photodynamic Therapy. *RSC Adv.* **2012**, *2*, 11169−11183.
(13) Stacey, O. J.; Pope, S. J. A. New Avenues in the Design and Potential Application of Metal Complexes for Photodynamic Therapy. *RSC Adv.* **2013**, *3*, 25550−25564.
(14) Kamkaew, A.; Lim, S. H.; Lee, H. B.; Kiew, L. V.; Chung, L. Y.; Burgess, K. BODIPY Dyes in Photodynamic Therapy. *Chem. Soc. Rev.* **2013**, *42*, 77−88.
(15) Zhao, J.; Wu, W.; Sun, J.; Guo, S. Triplet Photosensitizers: From Molecular Design to Applications. *Chem. Soc. Rev.* **2013**, *42*, 5323−5351.
(16) Gatri, R.; Ouerfelli, I.; Efrit, M. L.; Serein-Spirau, F.; Lère-Porte, J.-P.; Valvin, P.; Roisnel, T.; Bivaud, S.; Akdas-Kilig, H.; Fillaut, J.-L. Supramolecular Ruthenium−Alkynyl Multicomponent Architectures: Engineering, Photophysical Properties, and Responsiveness to Nitroaromatics. *Organometallics* **2014**, *33*, 665−676.
(17) Ceroni, P. Energy Up-Conversion by Low-Power Excitation: New Applications of an Old Concept. *Chem. - Eur. J.* **2011**, *17*, 9560−9564.
(18) Zhao, J.; Ji, S.; Guo, H. Triplet−Triplet Annihilation Based Upconversion: From Triplet Sensitizers and Triplet Acceptors to Upconversion Quantum Yields. *RSC Adv.* **2011**, *1*, 937−950.
(19) Hsu, H.-Y.; Vella, J. H.; Myers, J. D.; Xue, J.; Schanze, K. S. Triplet Exciton Diffusion in Platinum Polyyne Films. *J. Phys. Chem. C* **2014**, *118*, 24282−24289.
(20) Wu, W.; Guo, H.; Wu, W.; Ji, S.; Zhao, J. Organic Triplet Sensitizer Library Derived from a Single Chromophore (BODIPY) with Long-Lived Triplet Excited State for Triplet−Triplet Annihilation Based Upconversion. *J. Org. Chem.* **2011**, *76*, 7056−7064.
(21) Chen, Y.; Zhao, J.; Xie, L.; Guo, H.; Li, Q. Thienyl-Substituted Bodipys With Strong Visible Light-Absorption and Long-Lived Triplet Excited States as Organic Triplet Sensitizers for Triplet−Triplet Annihilation Upconversion. *RSC Adv.* **2012**, *2*, 3942−3953.
(22) Wu, W.; Zhao, J.; Sun, J.; Guo, S. Light-Harvesting Fullerene Dyads as Organic Triplet Photosensitizers for Triplet−Triplet Annihilation Upconversions. *J. Org. Chem.* **2012**, *77*, 5305−5312.
(23) Huang, L.; Zhao, J. C_{60}-Bodipy Dyad Triplet Photosensitizers as Organic Photocatalysts for Photocatalytic Tandem Oxidation/[3 + 2] Cycloaddition Reactions to Prepare Pyrrolo[2,1-*a*]Isoquinoline. *Chem. Commun.* **2013**, *49*, 3751−3753.
(24) Huang, L.; Cui, X.; Therrien, B.; Zhao, J. Energy-Funneling-Based Broadband Visible-Light-Absorbing Bodipy−C_{60} Triads and Tetrads as Dual Functional Heavy-Atom-Free Organic Triplet Photosensitizers for Photocatalytic Organic Reactions. *Chem. - Eur. J.* **2013**, *19*, 17472−17482.
(25) Huang, L.; Yu, X.; Wu, W.; Zhao, J. Styryl Bodipy-C_{60} Dyads as Efficient Heavy-Atom-Free Organic Triplet Photosensitizers. *Org. Lett.* **2012**, *14*, 2594−2597.
(26) Yang, P.; Wu, W.; Zhao, J.; Huang, D.; Yi, X. Using C_{60}-Bodipy Dyads That Show Strong Absorption of Visible Light and Long-Lived Triplet Excited States as Organic Triplet Photosensitizers for Triplet−Triplet Annihilation Upconversion. *J. Mater. Chem.* **2012**, *22*, 20273−20283.
(27) Huang, D.; Zhao, J.; Wu, W.; Yi, X.; Yang, P.; Ma, J. Visible-Light-Harvesting Triphenylamine Ethynyl C_{60}-BODIPY Dyads as Heavy-Atom-Free Organic Triplet Photosensitizers for Triplet-Triplet Annihilation Upconversion. *Asian J. Org. Chem.* **2012**, *1*, 264−273.
(28) Zhao, J.; Ji, S.; Wu, W.; Wu, W.; Guo, H.; Sun, J.; Sun, H.; Liu, Y.; Li, Q.; Huang, L. Transition Metal Complexes With Strong Absorption of Visible Light and Long-Lived Triplet Excited States: From Molecular Design to Applications. *RSC Adv.* **2012**, *2*, 1712−1728.
(29) Wu, W.; Zhao, J.; Guo, H.; Sun, J.; Ji, S.; Wang, Z. Long-Lived Room-Temperature Near-IR Phosphorescence of BODIPY in a Visible-Light-Harvesting $\hat{N}\hat{C}N$ Pt^{II}-Acetylide Complex with a Directly Metalated BODIPY Chromophore. *Chem. - Eur. J.* **2012**, *18*, 1961−1968.
(30) Sun, J.; Zhao, J.; Guo, H.; Wu, W. Visible-Light Harvesting Iridium Complexes as Singlet Oxygen Sensitizers for Photooxidation of 1,5-Dihydroxynaphthalene. *Chem. Commun.* **2012**, *48*, 4169−4171.
(31) Huang, L.; Zhao, J.; Guo, S.; Zhang, C.; Ma, J. Bodipy Derivatives as Organic Triplet Photosensitizers for Aerobic Photoorganocatalytic Oxidative Coupling of Amines and Photooxidation of Dihydroxylnaphthalenes. *J. Org. Chem.* **2013**, *78*, 5627−5637.
(32) Huang, L.; Zhao, J. Iodo-Bodipys as Visible-Light-Absorbing Dual-Functional Photoredox Catalysts for Preparation of Highly Functionalized Organic Compounds by Formation of C−C Bonds *Via* Reductive and Oxidative Quenching Catalytic Mechanisms. *RSC Adv.* **2013**, *3*, 23377−23388.
(33) Guo, S.; Ma, L.; Zhao, J.; Kücüköz, B.; Karatay, A.; Hayvali, M.; Yaglioglu, H. G.; Elmali, A. BODIPY Triads Triplet Photosensitizers Enhanced with Intramolecular Resonance Energy Transfer (RET): Broadband Visible Light Absorption and Application in Photooxidation. *Chem. Sci.* **2014**, *5*, 489−500.
(34) Guo, S.; Zhang, H.; Huang, L.; Guo, Z.; Xiong, G.; Zhao, J. Porous Material-Immobilized Iodo-Bodipy as an Efficient Photocatalyst for Photoredox Catalytic Organic Reaction to Prepare Pyrrolo[2,1-*A*]Isoquinoline. *Chem. Commun.* **2013**, *49*, 8689−8691.
(35) Ziessel, R.; Harriman, A. Artificial Light-harvesting Antennae: Electronic Energy Transfer by Way of Molecular Funnels. *Chem. Commun.* **2011**, *47*, 611−631.
(36) Fan, J.; Hu, M.; Zhan, P.; Peng, X. Energy Transfer Cassettes Based on Organic Fluorophores: Construction and Applications in Ratiometric Sensing. *Chem. Soc. Rev.* **2013**, *42*, 29−43.
(37) Bozdemir, O. A.; Erbas-Cakmak, S.; Ekiz, O. O.; Dana, A.; Akkaya, E. U. Towards Unimolecular Luminescent Solar Concentrators: Bodipy-Based Dendritic Energy-Transfer Cascade with Panchromatic Absorption and Monochromatized Emission. *Angew. Chem., Int. Ed.* **2011**, *50*, 10907−10912.

DOI: 10.1021/acs.jpca.5b03463
J. Phys. Chem. A 2015, 119, 6791−6806

(38) Zhang, X.; Xiao, Y.; Qian, X. Highly Efficient Energy Transfer in the Light Harvesting System Composed of Three Kinds of Boron−Dipyrromethene Derivatives. *Org. Lett.* **2008**, *10*, 29−32.
(39) Langhals, H.; Walter, A.; Rosenbaum, E.; Johansson, L. B.-Å. A Versatile Standard for Bathochromic Fluorescence Based on Intramolecular FRET. *Phys. Chem. Chem. Phys.* **2011**, *13*, 11055−11059.
(40) Vijayakumar, C.; Praveen, V. K.; Kartha, K. K.; Ajayaghosh, A. Excitation Energy Migration in Oligo(*p*-phenylenevinylene) Based Organogels: Structure-Property Relationship and FRET Efficiency. *Phys. Chem. Chem. Phys.* **2011**, *13*, 4942−4949.
(41) Sahoo, S. K.; Sharma, D.; Bera, R. K.; Crisponi, G.; Callan, J. F. Iron(III) Selective Molecular and Supramolecular Fluorescent Probes. *Chem. Soc. Rev.* **2012**, *41*, 7195−7227.
(42) Yu, X.; Jia, X.; Yang, X.; Liu, W.; Qin, W. Synthesis and Photochemical Properties of BODIPY-functionalized Silica Nanoparticles for Imaging Cu^{2+} in Living Cells. *RSC Adv.* **2014**, *4*, 23571−23579.
(43) Kostereli, Z.; Ozdemir, T.; Buyukcakir, O.; Akkaya, E. U. Tetrastyryl-BODIPY-Based Dendritic Light Harvester and Estimation of Energy Transfer Efficiency. *Org. Lett.* **2012**, *14*, 3636−3639.
(44) Zhang, C.; Zhao, J.; Wu, S.; Wang, Z.; Wu, W.; Ma, J.; Guo, S.; Huang, L. Intramolecular RET Enhanced Visible Light-Absorbing Bodipy Organic Triplet Photosensitizers and Application in Photooxidation and Triplet-Triplet Annihilation Upconversion. *J. Am. Chem. Soc.* **2013**, *135*, 10566−10578.
(45) Majumdar, P.; Yuan, X.; Li, S.; Le Guennic, B.; Ma, J.; Zhang, C.; Jacquemin, D.; Zhao, J. Cyclometalated Ir(III) Complexes with Styryl-BODIPY Ligands Showing Near IR Absorption/emission: Preparation, Study of Photophysical Properties and Application as Photodynamic/luminescence Imaging Materials. *J. Mater. Chem. B* **2014**, *2*, 2838−2854.
(46) Ma, J.; Yuan, X.; Kücüköz, B.; Li, S.; Zhang, C.; Majumdar, P.; Karatay, A.; Li, X.; Yaglioglu, H. G.; Elmali, A.; et al. Resonance energy transfer-enhanced rhodamine-styryl Bodipy dyad triplet photosensitizers. *J. Mater. Chem. C* **2014**, *2*, 3900−3913.
(47) Erbas-Cakmak, S.; Bozdemir, O. A.; Cakmak, Y.; Akkaya, E. U. Proof of Principle for a Molecular 1:2 Demultiplexer to Function as An Autonomously Switching Theranostic Device. *Chem. Sci.* **2013**, *4*, 858−862.
(48) Erbas-Cakmak, S.; Akkaya, E. U. Cascading of Molecular Logic Gates for Advanced Functions: A Self-Reporting, Activatable Photosensitizer. *Angew. Chem., Int. Ed.* **2013**, *52*, 11364−11368.
(49) Ziessel, R.; Allen, B. D.; Rewinska, D. B.; Harriman, A. Selective Triplet-State Formation during Charge Recombination in a Fullerene/Bodipy Molecular Dyad (Bodipy = Borondipyrromethene). *Chem. - Eur. J.* **2009**, *15*, 7382−7393.
(50) El-Khouly, M. E.; Amin, A. N.; Zandler, M. E.; Fukuzumi, S.; D'Souza, F. Near-IR Excitation Transfer and Electron Transfer in a BF_2-Chelated Dipyrromethane-Azadipyrromethane Dyad and Triad. *Chem. - Eur. J.* **2012**, *18*, 5239−5247.
(51) Xu, K.; Xie, Y.; Cui, X.; Zhao, J.; Glusac, K. D. DiiodoBodipy-Rhodamine Dyads: Preparation and Study of the Acid-Activatable Competing Intersystem Crossing and Energy Transfer Processes. *J. Phys. Chem. B* **2015**, *119*, 4175−4187.
(52) Mahmood, Z.; Xu, K.; Küçüköz, B.; Cui, X.; Zhao, J.; Wang, Z.; Karatay, A.; Yaglioglu, H. G.; Hayvali, M.; Elmali, A. DiiodoBodipy-Perylenebisimide Dyad/Triad: Preparation and Study of the Intramolecular and Intermolecular Electron/Energy Transfer. *J. Org. Chem.* **2015**, *80*, 3036−3049.
(53) Wu, S.; Zhong, F.; Zhao, J.; Guo, S.; Yang, W.; Fyles, T. Broadband Visible Light-Harvesting Naphthalenediimide (NDI) Triad: Study of the Intra-/Intermolecular Energy/Electron Transfer and the Triplet Excited State. *J. Phys. Chem. A* **2015**, *119*, 4787−4799.
(54) Ulrich, G.; Ziessel, R.; Harriman, A. The Chemistry of Fluorescent Bodipy Dyes: Versatility Unsurpassed. *Angew. Chem., Int. Ed.* **2008**, *47*, 1184−1201.
(55) Yogo, T.; Urano, Y.; Ishitsuka, Y.; Maniwa, F.; Nagano, T. Highly Efficient and Photostable Photosensitizer Based on BODIPY Chromophore. *J. Am. Chem. Soc.* **2005**, *127*, 12162−12163.
(56) Adarsh, N.; Shanmugasundaram, M.; Avirah, R. R.; Ramaiah, D. Aza-BODIPY Derivatives: Enhanced Quantum Yields of Triplet Excited States and the Generation of Singlet Oxygen and their Role as Facile Sustainable Photooxygenation Catalysts. *Chem. - Eur. J.* **2012**, *18*, 12655−12662.
(57) Adarsh, N.; Avirah, R. R.; Ramaiah, D. Tuning Photosensitized Singlet Oxygen Generation Efficiency of Novel Aza-BODIPY Dyes. *Org. Lett.* **2010**, *12*, 5720−5723.
(58) Bura, T.; Nastasi, F.; Puntoriero, F.; Campagna, S.; Ziessel, R. Ultrafast Energy Transfer in Triptycene-Grafted Bodipy Scaffoldings. *Chem. - Eur. J.* **2013**, *19*, 8900−8912.
(59) Brizet, B.; Eggenspiller, A.; Gros, C. P.; Barbe, J.-M.; Goze, C.; Denat, F.; Harvey, P. D. B,B-Diporphyrinbenzyloxy-BODIPY Dyes: Synthesis and Antenna Effect. *J. Org. Chem.* **2012**, *77*, 3646−3650.
(60) Guo, S.; Tao, R.; Zhao, J. Photoredox Catalytic Organic Reactions Promoted with Broadband Visible Light-absorbing Bodipyiodo-aza-Bodipy Triad Photocatalyst. *RSC Adv.* **2014**, *4*, 36131−36139.
(61) Apperloo, J. J.; Martineau, C.; van Hal, P. A.; Roncali, J.; Janssen, R. A. J. Intra- and Intermolecular Photoinduced Energy and Electron Transfer between Oligothienylenevinylenes and N-Methylfulleropyrrolidine. *J. Phys. Chem. A* **2002**, *106*, 21−31.
(62) Baruah, M.; Qin, W.; Flors, C.; Hofkens, J.; Vallée, R. A. L.; Beljonne, D.; Van der Auweraer, M.; De Borggraeve, W. M.; Boens, N. Solvent and pH Dependent Fluorescent Properties of a Dimethylaminostyryl Borondipyrromethene Dye in Solution. *J. Phys. Chem. A* **2006**, *110*, 5998−6009.
(63) Yuan, M.; Yin, X.; Zheng, H.; Ouyang, C.; Zuo, Z.; Liu, H.; Li, Y. Light Harvesting and Efficient Energy Transfer in Dendritic Systems: New Strategy for Functionalized Near-Infrared BF_2-Azadipyrromethenes. *Chem. - Asian J.* **2009**, *4*, 707−713.
(64) Zhang, J.; Fischer, M. K. R.; Bäuerle, P.; Goodson, T. Energy Migration in Dendritic Oligothiophene-Perylene Bisimides. *J. Phys. Chem. B* **2013**, *117*, 4204−4275.
(65) Rurack, K.; Kollmannsberger, M.; Daub, J. Molecular Switching in the Near Infrared (NIR) with a Functionalized Boron−Dipyrromethene Dye. *Angew. Chem., Int. Ed.* **2001**, *40*, 385−387.
(66) Lazarides, T.; Charalambidis, G.; Vuillamy, A.; Réglier, M.; Klontzas, E.; Froudakis, G.; Kuhri, S.; Guldi, D. M.; Coutsolelos, A. G. Promising Fast Energy Transfer System via an Easy Synthesis: Bodipy−Porphyrin Dyads Connected via a Cyanuric Chloride Bridge, Their Synthesis, and Electrochemical and Photophysical Investigations. *Inorg. Chem.* **2011**, *50*, 8926−8936.
(67) Whited, M. T.; Djurovich, P. I.; Roberts, S. T.; Durrell, A. C.; Schlenker, C. W.; Bradforth, S. E.; Thompson, M. E. Singlet and Triplet Excitation Management in a Bichromophoric Near-Infrared-Phosphorescent BODIPY-Benzoporphyrin Platinum Complex. *J. Am. Chem. Soc.* **2011**, *133*, 88−96.
(68) Sabatini, R. P.; McCormick, T. M.; Lazarides, T.; Wilson, K. C.; Eisenberg, R.; McCamant, D. W. Intersystem Crossing in Halogenated Bodipy Chromophores Used for Solar Hydrogen Production. *J. Phys. Chem. Lett.* **2011**, *2*, 223−227.
(69) Lazarides, T.; McCormick, T. M.; Wilson, K. C.; Lee, S.; McCamant, D. W.; Eisenberg, R. Sensitizing the Sensitizer: The Synthesis and Photophysical Study of Bodipy-Pt(II)(diimine)(dithiolate) Conjugates. *J. Am. Chem. Soc.* **2011**, *133*, 350−364.
(70) Rachford, A. A.; Ziessel, R.; Bura, T.; Retailleau, P.; Castellano, F. N. Boron Dipyrromethene (Bodipy) Phosphorescence Revealed in $[Ir(ppy)_2(bpy\text{-}C{\equiv}C\text{-}Bodipy)]^+$. *Inorg. Chem.* **2010**, *49*, 3730−3736.
(71) Hofmann, C. C.; Lindner, S. M.; Ruppert, M.; Hirsch, A.; Haque, S. A.; Thelakkat, M.; Köhler, J. Mutual Interplay of Light Harvesting and Triplet Sensitizing in a Perylene Bisimide Antenna−Fullerene Dyad. *J. Phys. Chem. B* **2010**, *114*, 9148−9156.
(72) Zheng, G.; Chen, J.; Stefflova, K.; Jarvi, M.; Li, H.; Wilson, B. C. Photodynamic Molecular Beacon as an Activatable Photosensitizer Based on Protease-controlled Singlet Oxygen Quenching and Activation. *Proc. Natl. Acad. Sci. U. S. A.* **2007**, *104*, 8989−8994.

DOI: 10.1021/acs.jpca.5b03463
J. Phys. Chem. A 2015, 119, 6791−6806

(73) Bugaj, A. M. Targeted Photodynamic Therapy − a Promising Strategy of Tumor Treatment. *Photochem. Photobiol. Sci.* **2011**, *10*, 1097−1109.
(74) Ozlem, S.; Akkaya, E. U. Thinking Outside the Silicon Box: Molecular AND Logic As an Additional Layer of Selectivity in Singlet Oxygen Generation for Photodynamic Therapy. *J. Am. Chem. Soc.* **2009**, *131*, 48−49.
(75) Cakmak, Y.; Kolemen, S.; Duman, S.; Dede, Y.; Dolen, Y.; Kilic, B.; Kostereli, Z.; Yildirim, L. T.; Dogan, A. L.; Guc, D.; et al. Designing Excited States: Theory-Guided Access to Efficient Photosensitizers for Photodynamic Action. *Angew. Chem.* **2011**, *123*, 12143−12147.
(76) Fukuzumi, S.; Ohkubo, K. Selective Photocatalytic Reactions with Organic Photocatalysts. *Chem. Sci.* **2013**, *4*, 561−574.
(77) Merkel, P. B.; Dinnocenzo, J. P. Thermodynamic energies of donor and acceptor triplet states. *J. Photochem. Photobiol., A* **2008**, *193*, 110−121.
(78) Ford, W. E.; Kamat, P. V. Photochemistry of 3,4,9,10-Perylenetetracarboxylic Dianhydride dyes. 3. Singlet and Triplet Excited-State Properties of the Bis(2,5-di-*tert*-butylphenyl)imide Derivative. *J. Phys. Chem.* **1987**, *91*, 6373−6380.
(79) Majumdar, P.; Nomula, R.; Zhao, J. Activatable Triplet Photosensitizers: Magic Bullets for Targeted Photodynamic Therapy. *J. Mater. Chem. C* **2014**, *2*, 5982−5997.
(80) EI-Khouly, M. E.; Fukuzumi, S. Light Harvesting Phthalocyanine/Subphthalocyanine System: Intermolecular Electron-Transfer and Energy-Transfer Reactions *via* the Triplet Subphthalocyanine. *J. Porphyrins Phthalocyanines* **2011**, *15*, 111−117.
(81) Turro, N. J.; Ramamurthy, V.; Scaiano, J. C. *Principles of Molecular Photochemistry: An Introduction*; University Science Books: Sausalito, CA, 2009.
(82) Feng, K.; Yu, M.-L.; Wang, S.-M.; Wang, G.-X.; Tung, C.-H.; Wu, L.-Z. Photoinduced Triplet-Triplet Energy Transfer in a 2-Ureido-4(1*H*)-Pyrimidinone-Bridged, Quadruply Hydrogen-Bonded Ferrocene-Fullerene Assembly. *ChemPhysChem* **2013**, *14*, 198−203.
(83) Lakowicz, J. R. *Principles of Fluorescence Spectroscopy*, 2nd ed.; Kluwer Academic: New York, 1999.

DOI: 10.1021/acs.jpca.5b03463
J. Phys. Chem. A 2015, 119, 6791−6806